JOURNAL OF MATERIALS SCIENCE 16 (1981) 2337–2359

Review
Corrosion behaviour of metallic glasses

Y. WASEDA, K. T. AUST
Department of Metallurgy and Materials Science, University of Toronto, Toronto, Canada

A review is presented concerning the current experimental information on the corrosion behaviour of metallic glasses, particularly of iron-base glasses of metal–metalloid-type obtained by using electrochemical measurements and scanning electron microscopy. The corrosion characteristics of glasses of metal–metal-type, such as Cu–Ti, are also compared with those of known, highly corrosion-resistant metallic glasses. Compositional and structural effects, such as the addition of metallic or metalloid elements, amorphous phase structure effects, passive film formation and stress corrosion cracking, are also discussed.

1. Introduction

Rapidly-quenched alloys with structural characteristics similar to glass are mainly composed of metallic elements, in contrast to the composition of oxide and chalcogenide glasses. These glass-like alloys are termed "metallic glasses" since their electrical and mechanical properties are similar to those of metals. Since the first report of unusual structures obtained by rapid-quenching from the melt, by Klement *et al.* [1], many studies on the structure and properties of metallic glasses have been conducted. As a result, several metallic glasses have recently passed from the laboratory stage to become useful new engineering materials in applications from power transformer cores to magnetic tape heads for tape recorders. As a result of the increasing interest in this field, specialized monographs and review articles on this relatively new class of non-crystalline materials have been published, e.g., [2]. However, very little attention has been given to a detailed description of the chemical properties, such as corrosion behaviour, of these metallic glasses in terms of both a fundamental and an engineering point of view. The subject of the corrosion of metallic glasses is of great interest since it has been discovered that several iron-base metallic glasses possess corrosion-resistance properties superior to those of crystalline alloys of stainless steel [3].

An attempt has been made in this paper, for the above reasons, to review the experimental information on the corrosion behaviour of metallic glasses. Studies in this field have been most extensively carried out by Masumoto and co-workers, and, thus, the present review draws mainly from their results, but includes some recent information obtained by the present authors.

2. Fundamental features of the corrosion behaviour of metallic glasses

In 1974, Naka, Hasimoto and Masumoto [3] reported the first results on the corrosion behaviour of metallic glasses. Fig. 1 shows a comparison of the corrosion rates in HCl with various concentrations at 30° C of metallic glasses of Fe–$Cr_{10}P_{13}C_7$ and Fe–$Cr_{10}Ni_5P_{13}C_7$ (all compositions in this paper are expressed in atomic per cent by subscripts), and a typical high corrosion-resistant material of 18-8 stainless steel (AISI 304). The corrosion rates were estimated from the weight losses after immersion for the period from 46 to 144 h in the case of 18-8 stainless steel and for 168 h for the metallic glasses. The results shown in Fig. 1 are taken from works conducted under similar experimental conditions by Naka *et al.* [3] and Waseda and Aust [4], and the results show good agreement. A large weight loss was detected in the crystalline 18-8 stainless steel mainly due to the usual pitting-corrosion produced by the HCl solution. However, the alloy glasses showed no measurable weight

0022–2461/81/092337–23$04.30/0

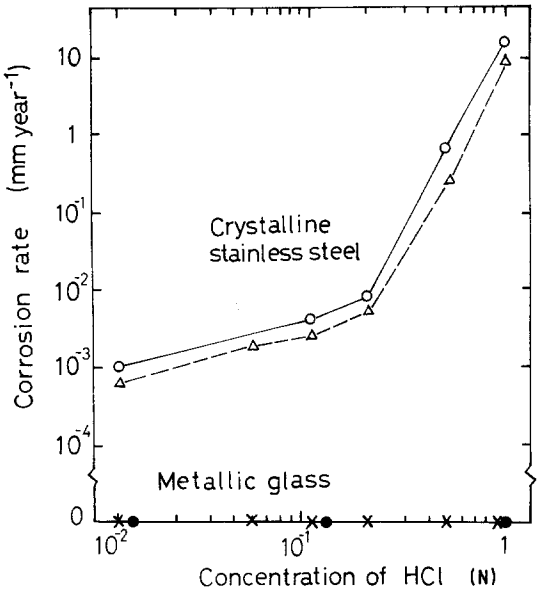

Figure 1 Comparison of the corrosion rates of metallic glasses and crystalline stainless steel as a function of HCl concentration at 30° C [3]. No weight changes of the metallic glasses of $Fe–Cr_{10}P_{13}C_7$ were detected by a microbalance after immersion for 200 h. (○, ● [3]; ×, △ [4]).

change on a microbalance after immersion for 168 h. In addition, no detectable change was observed on the surface of the alloy glasses after immersion for 168 h in the HCl concentration range presently investigated. The distinct difference observed in these results concerning the crystalline and amorphous states may be interpreted as follows. Pitting and grain-boundary corrosion occur in the crystalline stainless steel in solutions containing Cl^- ions and, thus, a large weight loss was observed in the crystalline state. However, such corrosion was almost non-observable in the glassy state with HCl solution. As shown in Table I, a similar observation has been noted from recent results [4] of immersion tests in 10 wt% $FeCl_3 \cdot 6H_2O$ solutions which have frequently been used for pitting corrosion tests of conventional stainless steels. The crystalline 18-8 stainless steel shows a high corrosion rate due to pitting corrosion in $FeCl_3$ solution. The 316-type stainless steel shows a lower corrosion rate. On the other hand, the alloy glasses exhibited almost no weight change after immersion for 200 h in $FeCl_3$ solutions.

Fig. 2 gives the corrosion-rate dependence on the Cr-content estimated from measurements of weight losses in 1 N NaCl solution at 30° C for both crystalline and amorphous Fe–Cr alloys [3].

TABLE I Corrosion rates* of metallic glasses and crystalline stainless steel in 10 wt% $FeCl_3 \cdot 6H_2O$ solution at 60° C

Specimen	Corrosion rate (mm year^{-1})	Reference
Metallic glasses		
$Fe–Cr_8P_{13}C_7$	*	[3]
$Fe–Cr_{10}P_{13}C_7$	*	[2]
$Fe–Cr_{10}Ni_5P_{13}C_7$	*	[3]
$Fe–Cr_{10}P_{13}C_7$	*	[4]
$Fe–Cr_{10}N_{10}P_{13}C_7$	*	[4]
Crystalline stainless steel†		
304-type (18Cr–8Ni)	120.0	[3]
136-type (17Cr–12Ni–2.5Mo)	27.5	[3]
304-type (18Cr–8Ni)	138	[4]
316-type (17Cr–12Ni–2.5Mo)	39.4	[4]

*No weight change of metallic glasses was observed using a microbalance after an immersion test for 200 h.
†Corrosion rates of 304-type and of 316-type strainless steels were estimated from weight change after immersion tests for 20 h and 200 h, respectively.

The corrosion rate of the crystalline alloys is relatively insensitive to the Cr-content in a non-oxidizing corrosive NaCl solution. The results shown in Fig. 2 indicate that the $Fe–P_{13}C_7$ alloy glasses are rapidly corroded at a corrosion rate much higher than that of crystalline pure iron;

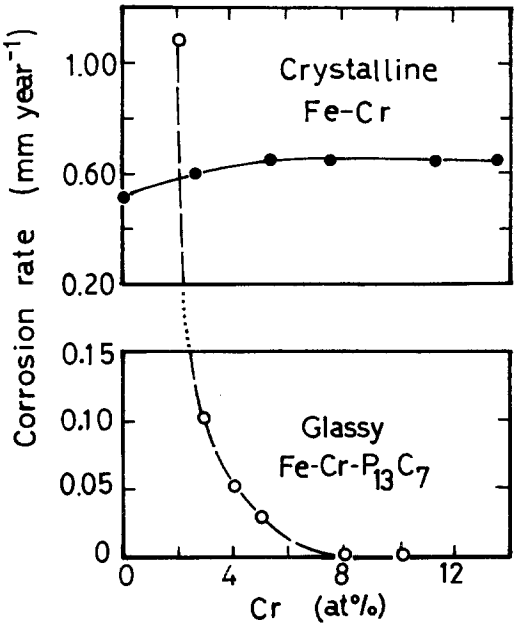

Figure 2 Comparison of the corrosion rates of glassy $Fe–Cr–P_{13}C_7$ alloys and crystalline Fe–Cr alloys in 1 N NaCl solution at 30° C [3].

however, the corrosion rates are lower than those of crystalline Fe–Cr alloys with an addition of 2 at% Cr or more and the composition in which iron was progressively replaced by Cr became exceedingly resistant to electrolytic corrosion at a Cr-content of about 8 at% and more, even after immersion for 168 h.

Corrosion characteristics were also studied using electrochemical measurements. Fig. 3 gives the potentiostatic polarization curves of the glass of $Fe–Cr_{10}P_{13}C_7$ in both 1 M H_2SO_4 and 1 N NaCl solutions [3]. These measurements were made after polarization for 1 h at individual potentials. No anodic current higher than 10^{-7} A cm^{-2} was observed over the wide range from the corrosion potential to the neighbourhood of the transpassive potential. This suggests that passivation of this alloy glass takes place spontaneously upon immersion in solutions and explains why no weight change is observed even after a long period of immersion in both acidic and neutral solutions.

The corrosion behaviour of Ni-base [5] and Co-base [6] alloy glasses has been found to be quite similar to those of the Fe-base alloy glasses mentioned above. Again the corrosion rate decreases remarkably with an increase in the Cr-content, as exemplified by the results of $Ni–Cr–P_{15}B_5$ glasses, shown in Fig. 4 [5]; compositions with about 8 at% Cr are practically immune, since these glasses do not suffer pitting corrosion in 10 wt% $FeCl_3 \cdot 6H_2O$ solution at 30° C. On the polarization curves, no active state is observed by spontaneous passivation and the corrosion potentials are in the passive region of Cr as shown in Fig. 5 [5]. The alloy glasses containing about 8 at% Cr show a wide passive region and a critical pitting corrosion potential does not appear, even in a 1 N HCl solution.

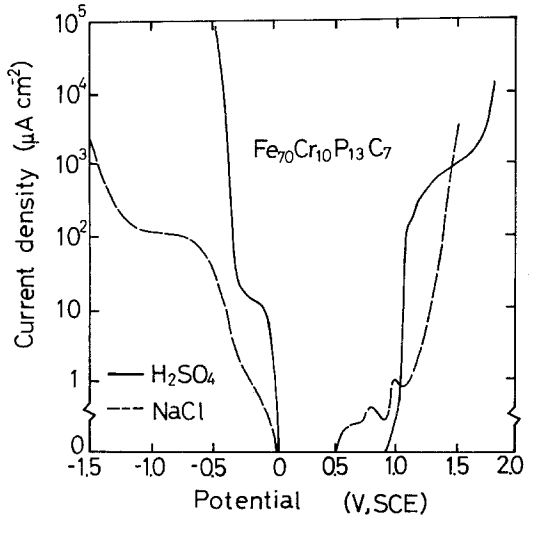

Figure 3 Potentiostatic polarization curves of glassy $Fe–Cr_{10}P_{13}C_7$ in 1 M H_2SO_4 and 1 N NaCl solution [3].

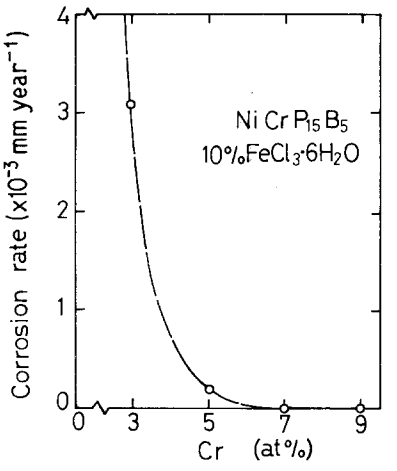

Figure 4 Plot of corrosion rates of metallic glasses of $Ni–Cr–P_{15}B_5$ in 10 wt% $FeCl_3 \cdot 6H_2O$ at 30° C against Cr-content [5].

These interesting results, first reported by Masumoto and co-workers, clearly indicate that an addition of about 8 at% Cr to glass-forming Fe-base, Ni-base and Co-base alloys with metalloid elements such as P and C as one of the constituents evidently inhibits the corrosion rate of metallic glasses in both acidic and neutral solutions. Thus it appears that the use of metallic glasses with compositions similar to conventional stainless steel may be a solution to the corrosion problems in metallic alloys.

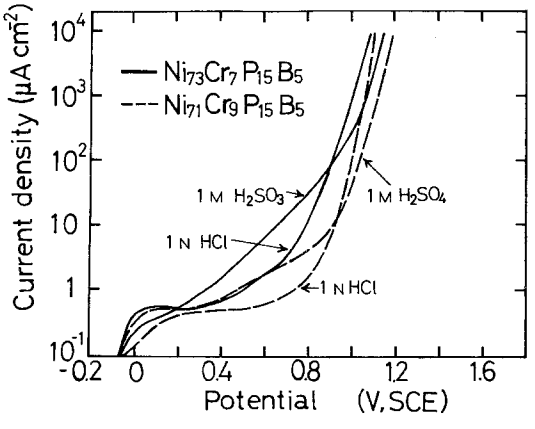

Figure 5 Potentiostatic polarization curves of metallic glasses of $Ni–Cr–P_{15}B_5$ in 1 M H_2SO_4 and 1 N HCl solutions [5].

3. Recent corrosion study of iron, nickel and cobalt base glasses by electrochemical measurements and scanning electron microscopy

Following the first work by Naka, Hashimoto and Masumoto [3], there have been many studies on the corrosion behaviour of metallic glasses. However, it is evident that further understanding is required concerning the relative importance of amorphous structure and elemental composition in the corrosion resistance of metallic glasses. From this point of view, the corrosion behaviour of several Fe–Ni–B glasses has recently been investigated by electrochemical measurements and scanning electron microscopy [7]. This work was conducted in order to compare the corrosion characteristics of Fe–Ni–B glasses with those of known highly corrosion-resistant glasses of $Fe–Cr_{10}P_{13}C_7$ and $Fe–Cr_{10}Ni_{10}P_{13}C_7$. The Fe–Ni–B glasses are of particular importance in the field of practical application of metallic glasses since the Fe–B-base glasses show interesting properties such as a large saturation magnetization and Invar characteristics, see for example [8].

Work on these metallic glasses was preceded by experiments to determine the feasibility of using conventional corrosion test equipment to measure the surface potential against current density characteristics for samples of very small size, since generally the glassy samples are in the shape of ribbon of about 1–3 mm width and 0.03 mm thickness. The effect of specimen size on the potentiodynamic polarization measurements was studied using crystalline 304-type stainless steel in the solution-treated condition. As shown in Table II, the polarization tests in 1 N H_2SO_4 on crystalline specimens with six different exposed surface areas between 3.6 and 9.5 cm^2 showed no influence of specimen size on such measurements, thus providing some evidence that very small size specimens of metallic glasses could justifiably be used in corrosion studies.

TABLE II Measured surface area and polarization curve parameters for crystalline 304-type stainless steel to test the effect of specimen size on potentiodynamic polarization measurements in a 1 N H_2SO_4 solution [7]

Specimen number	Surface area exposed (cm^2)	Corrosion potential (V)	Primary passive potential (V)
1	9.471	−0.335	−0.30
2	5.998	−0.329	−0.30
3	5.651	−0.322	−0.30
4	4.276	−0.335	−0.30
5	4.231	−0.343	−0.31
6	3.623	−0.347	−0.31

Fig. 6 shows a recently obtained [7] potentiodynamic polarization curve (Curve a) for the $Fe–Cr_{10}P_{13}C_7$ glass together with the first results (Curve b), obtained in 1974 [3]. A nitrogen atmosphere and an applied potential scanning rate of 0.6 $V h^{-1}$ was used in the experiments for Curve a, whereas Naka *et al.* [3] conducted their potentiodynamic polarization tests in air and at a potential scanning rate of 8.52 $V h^{-1}$. The basic profiles of both Curves a and b in Fig. 6 are quite similar and Curve a closely approached the current density values of Curve b, illustrating the good corrosion resistance properties of the $Fe–Cr_{10}P_{13}C_7$ glass. The active region is almost non-existent and leads directly into a passive region, indicating that a highly uniform passive film is formed very quickly. The corrosion resistance of this alloy is attributed partly to the formation of a passive film of hydrated chromium oxyhydroxides [9] with a high protective quality associated with the

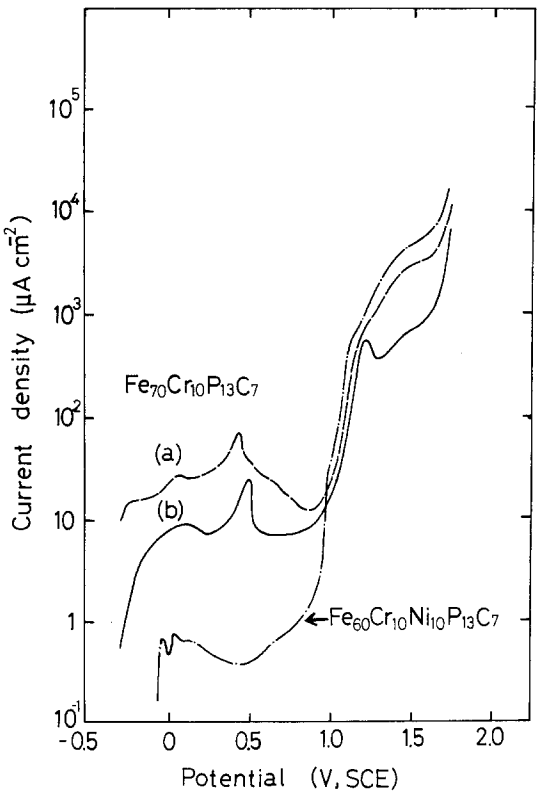

Figure 6 Potentiodynamic polarization curves of metallic glasses of $Fe–Cr_{10}P_{13}C_7$ and $Fe–Cr_{10}Ni_{10}P_{13}C_7$ measured in 2 N H_2SO_4 solution at 30° C (a: [7]; b: [3]).

presence of Cr and P, based on the suggestion by Naka *et al.* [10]. The potentiodynamic polarization curve for the Fe–$Cr_{10}Ni_{10}P_{13}C_7$ glass is also given in Fig. 6, indicating the remarkable corrosion resistance properties of this alloy glass. There is essentially no active region and a passive film is formed rapidly and at a much lower current density than that of the Fe–$Cr_{10}P_{13}C_7$ glass. This suggests that the addition of Ni to the Fe–$Cr_{10}P_{13}C_7$ glass results in the formation of a passive film of even greater uniformity and stability. The addition of Ni is considered to promote the formation of a passive film in the presence of Cr [11].

Fig. 7 gives the potentiodynamic polarization curves for a series of four Fe–Ni–B glasses with different boron contents (14, 16, 22, and 24 at %) and the same Ni/Fe ratio of 0.6 in each alloy. Due to the high dissolution rates the complete anodic polarization curves were not obtained. These curves clearly show that these glasses actively corroded. Their behaviour appears to be very similar to that of the $Fe_{80}P_{13}C_7$ glass without Cr, which dissolves actively in a 1 N NaCl solution at 30° C without showing anodic passivation [3]. The rapid dissolution of metal at the epoxy coating interface on the working electrode is attributed to crevice corrosion. The potentiodynamic polarization curve for the $Fe_{20}Ni_{60}B_{20}$ glass is also given in Fig. 7. In spite of the high Ni-content, being much higher with a Ni/Fe ratio of 3, the same poor corrosion resistance properties are still evident. A high dissolution rate of the metal at the coating interface again resulted in crevice corrosion for the $Fe_{20}Ni_{60}C_{20}$ glass. This contrasts with the case of the Fe–P–C-type glasses in which the addition of Ni improves their corrosion resistance in 2 N H_2SO_4 solution [11]. Crevice corrosion did not occur in the glasses of Fe–$Cr_{10}P_{13}C_7$ and Fe–$Cr_{10}Ni_{10}P_{13}C_7$, whose working electrodes were prepared in the exact same manner as for the Fe–Ni–B glasses. Experiments with an artificial crevice cell indicated that amorphous Fe–Ni–Cr–P–B alloys can be forced to crevice corrode but only at very anodic or transpassive potentials [12]. The occurrence of crevice corrosion in the Fe–Ni–B glasses can not, therefore, be attributed entirely to the working electrode design or to the sample preparation technique. The poor corrosion resistance properties must be related to their elemental composition, i.e., the absence of elements such as Cr and P.

The morphologies of metallic glasses were also

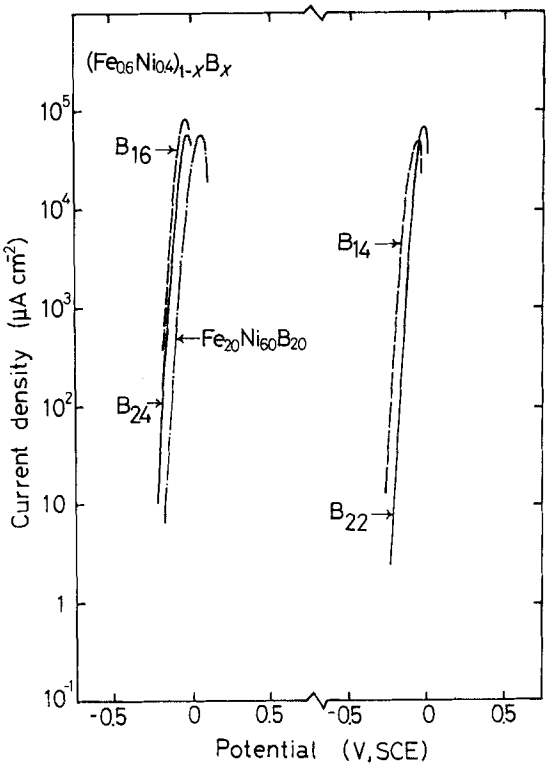

Figure 7 Potentiodynamic polarization curves of metallic glasses of Fe–Ni–B alloys with Ni/Fe = 0.5 and B = 14, 16.22 and 24 at % and $Fe_{20}Ni_{60}B_{20}$ in 2 N H_2SO_4 solution at 30° C [7].

studied using scanning electron microscopy. Fixed potential tests were performed in order to prepare the glassy samples for SEM examination. The desired fixed potentials were chosen from the potentiodynamic polarization curves according to the region of interest, active, passive or transpassive regions. Scanning electron micrographs of the Fe–$Cr_{10}P_{13}C_7$ glass are shown in Fig. 8. The micrograph in Fig. 8a corresponds to the "as-quenched" sample, i.e., the sample before a polarization test. The glassy samples have a rough surface on one side, as seen in Fig. 8a, and a smooth surface on the other side. This is due to the use of a quenching technique of the single-roller type [2]; the rough surface corresponds to the surface in contact with the roller, which is rotated at a high speed. Fig. 8b and c correspond to a sample of the same glass which was held at a constant potential of 0.875 V in the passive region for 1.5 h and a sample of the glass which was held at a constant potential of 1.15 V in the transpassive region for 1.5 h, respectively. The entirely different surface morphology seen in Fig. 8c compared with that seen in Fig. 8a and b, implies the formation of a

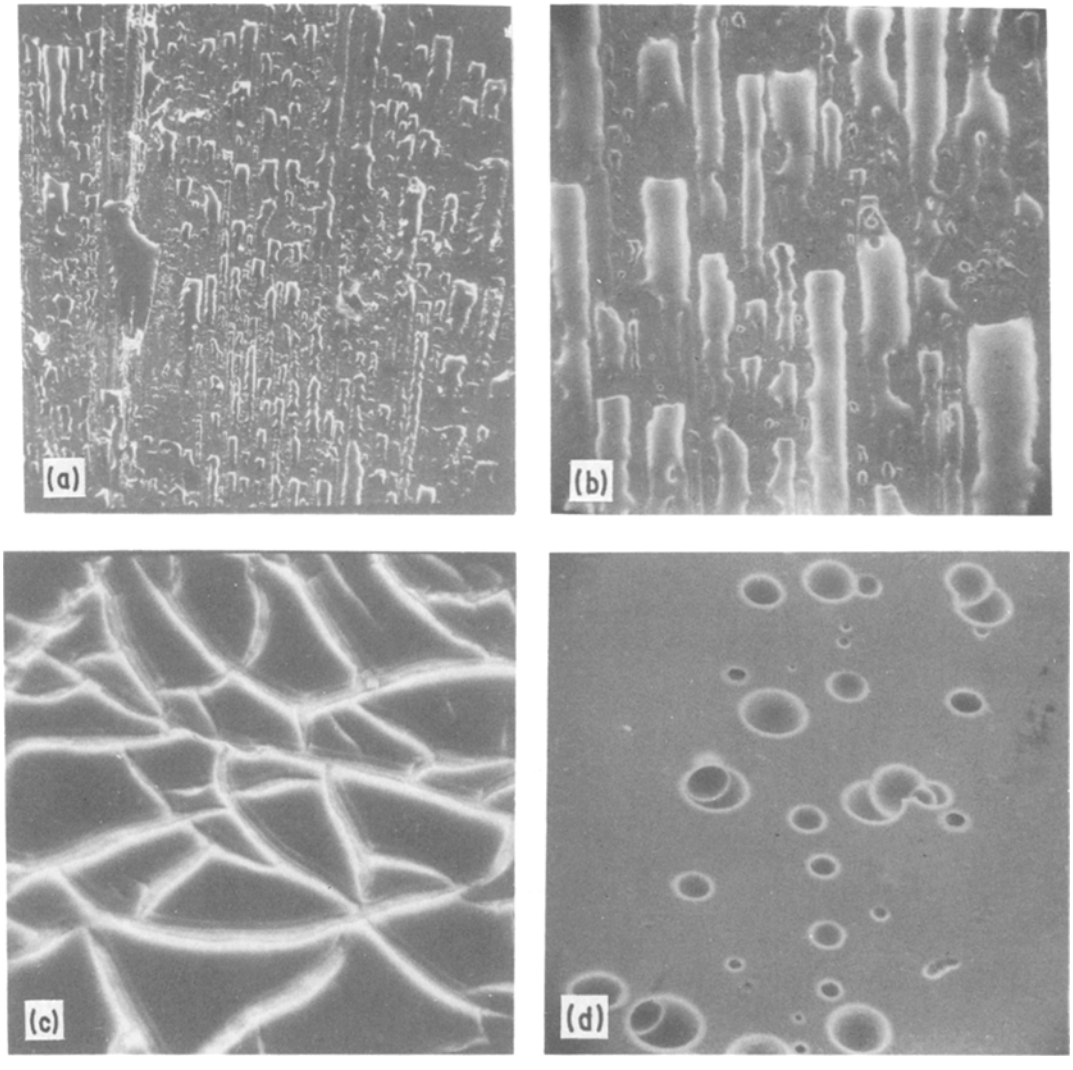

Figure 8 Scanning electron micrographs of amorphous $Fe_{70}Cr_{10}P_{13}C_7$ alloy [7]. (a) "As-quenched" condition before corrosion test, × 245; (b) held at 0.875 V against SCE (passive region) for 1.5 h, × 645; (c) held at 1.15 V against SCE (transpassive) for 1.5 h showing break-down of passive film, × 6100; (d) after polarization test up to 1.75 V against SCE, showing pitting attack, × 2025.

passive film and its break-down. Pitting corrosion has been reported to be almost non-existent in metallic glasses such as $Fe–Cr_{10}P_{13}C_7$ when exposed to chloride solutions [3]. However, Fig. 8d depicts the glass subjected to a full potentiodynamic polarization test up to 1.75 V in the H_2SO_4 solution; evidence of pitting-corrosion attack is suggested which is related to the rapid increase in current density (see Fig. 6) during transpassive dissolution.

Similar SEM studies were also performed for the $Fe–Cr_{10}Ni_{10}P_{13}C_7$ glass. Fig. 9a shows the glassy sample before a polarization test, again indicating a rough surface on one side. Fig. 9b and c illustrate samples of the $Fe–Cr_{10}Ni_{10}P_{13}C_7$ glass which were held at a constant potential of 0 V in the active region for 1.5 h and at 0.37 V in the passive region for 1.5 h, respectively. Very little corrosion attack, if any, can be seen. However, pitting-corrosion is again revealed, as shown in Fig. 9d for the same glass subjected to a full potentiodynamic polarization test up to 1.75 V.

The corrosion behaviour of several Fe–Si–B, Ni–Si–B and Co–Fe–Si–B glasses has also been investigated by electrochemical measurements [13]. As shown in Fig. 10, using the results of $Fe_{83}Si_5B_{12}$ and $Fe_{83}Si_7B_{10}$ as an example, the potentiodynamic polarization curves indicate that

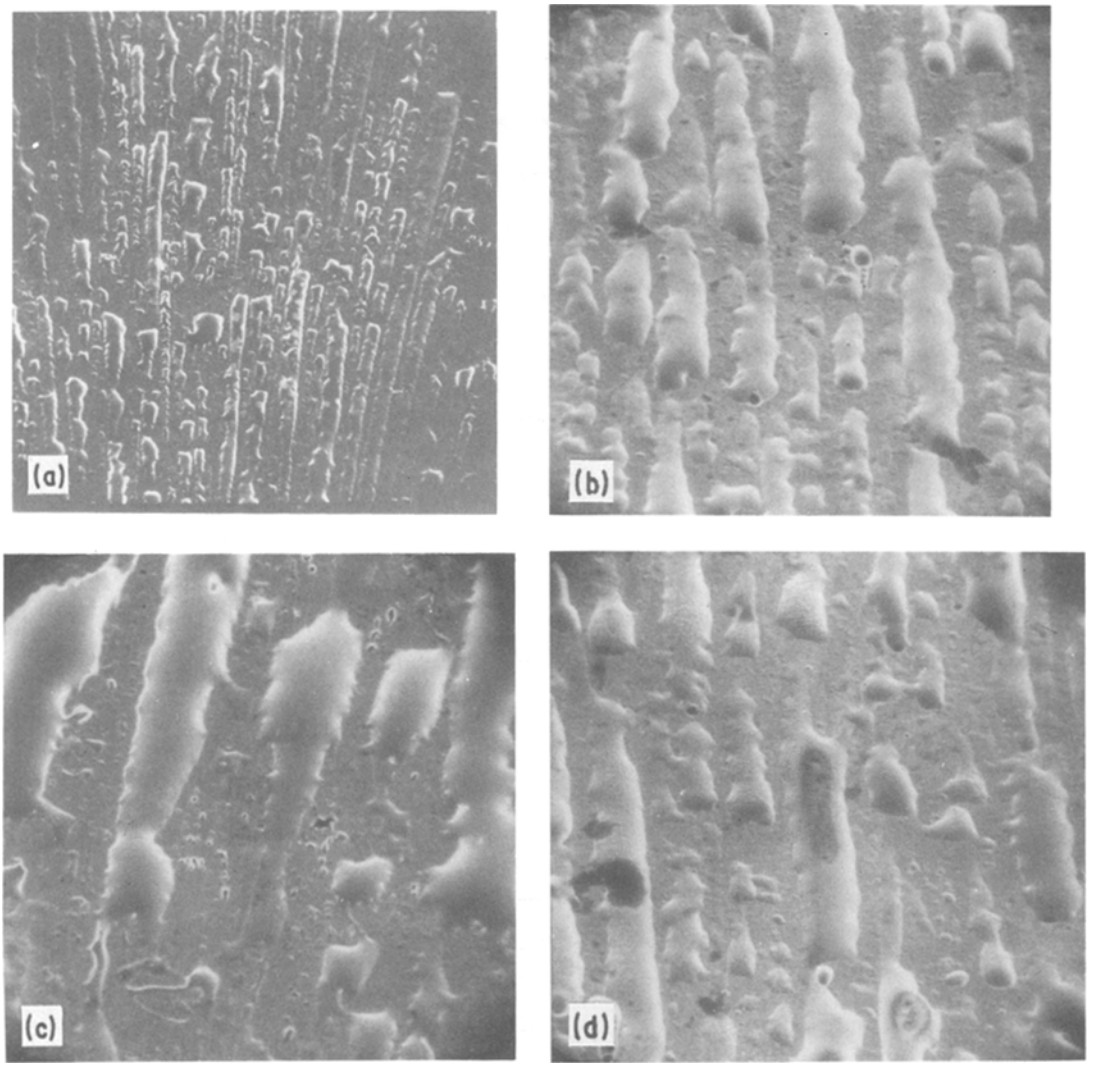

Figure 9 Scanning electron micrographs of amorphous $Fe_{60}Cr_{10}Ni_{10}P_{13}C_7$ alloy [7]. (a) "As-quenched" condition before corrosion test, × 240; (b) held at 0 V against SCE (active region) for 1.5 h, × 640; (c) held at 0.37 V against SCE (passive) for 1.5 h, × 1125; (d) after polarization test up to 1.75 V against SCE showing pitting attack, × 645.

these alloy glasses actively corroded without showing anodic passivation. Similar results were also observed in the Ni–Si–B alloys and the Co–Fe–Si–B alloy [13] under the present environmental test condition (in 0.1 and 1.0 N H_2SO_4 solution and at a potential scanning rate of 0.6 V h^{-1} and 3.0 V h^{-1}). Due to the rapid dissolution rate of the alloy glasses at the epoxy coating interface on the working electrode, attributed to crevice corrosion, the complete anodic polarization curves were not obtained under the test conditions stated above. However, it should be noted that the Ni–Si–B and Ni–Cu–Si–B alloy glasses survived the corrosion test to an applied potential of only 0.25 V (Saturated calomel electrode, SCE) when the following condition was used: in 1.0 N H_2SO_4 solution at a potential scanning rate of 0.6 V h^{-1} [13].

A more noble corrosion potential, E_{corr}, for Ni–Si–B (about −0.25 V) as compared to that of Fe–Si–B (about −0.5 V) was observed since nickel is more noble than iron. It appears that the observed poor corrosion resistance of Fe–Si–B and Ni–(Cu)–Si–B glasses in H_2SO_4 solutions must be related to their elemental composition, i.e., the lack of elements such as Cr and P. Also, a Si concentration of up to 8 at % in these alloys does not provide passivation. The absence of grain boundaries, segregates or crystalline defects alone

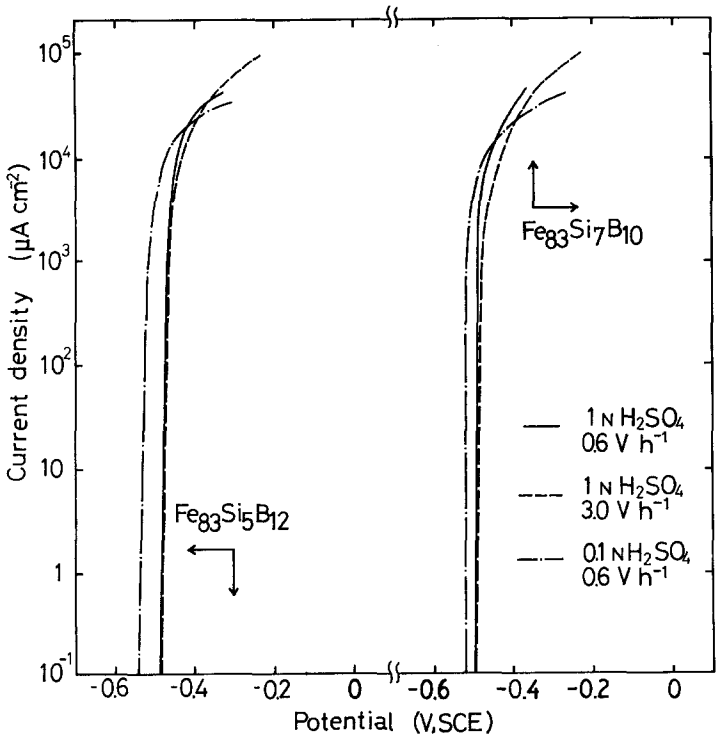

Figure 10 Potentiodynamic polarization curves of amorphous (a) $Fe_{83}Si_5B_{12}$ and (b) $Fe_{83}Si_7B_{10}$ alloys in 0.1 N and 1.0 N H_2SO_4 at potential scan rates of 0.6 V h^{-1} and 3.0 V h^{-1} [13].

in such glasses is evidently not sufficient to give good corrosion resistance.

Fig. 11 illustrates the effect of varying Cr additions on the potentiodynamic polarization behaviour of the Co–Fe–Si–B glasses. This alloy glass is of importance in the application of metallic glasses in magnetic tape heads for tape recorders, for example [8]. It is apparent from Fig. 11 that increasing the Cr-content from 3 to 7.5 at% produces a marked improvement in the corrosion resistance of these alloy glasses in 1 N H_2SO_4 at 30° C. The Co–Fe–Si–B glasses with no Cr addition did not passivate and behaved in a manner similar to that of the Fe–Si–B and Ni–Si–B glasses previously discussed.

The minimum passive current density, I_p, decreases with increasing Cr-content, reaching a value of about 10 $\mu A\,cm^{-2}$ with 7.5 at% Cr (Fig. 11). This low passive current density is similar to that previously obtained for the $Fe_{70}Cr_{10}P_{13}C_7$ alloy in 2 N H_2SO_4 (Fig. 6). However, the critical anodic current density, I_c, of the Co–Fe–Si–B alloy containing 7.5 at% Cr is higher (about 10^3 $\mu A\,cm^{-2}$), indicating a slower formation of the passive film. The presence of P in metallic glasses stimulates the active dissolution of the alloy resulting in a rapid enrichment of trivalent chromium ion in the bulk material–solution interface and in a rapid formation of the chromium-enriched passive film [14]. However, B and Si do not accelerate the dissolution and are partly present in the passive film as silicate or borate which hinder the chromium enrichment in the passive film. For example, in one study [15] of $Co_{70}Cr_{10}B_{20}$ and $Co_{70}Cr_{10}P_{20}$ it was found that the boron-containing alloy had a higher corrosion rate and did not passivate because the film contained a significant borate content; however, the phosphorus-containing alloy passivated readily.

A comparison of the potentiodynamic polarization curves obtained in 0.1 N H_2SO_4 at a potential scan rate of 6.0 V h^{-1} is presented in Fig. 12 for the Fe–Ni–Cr–Si–B alloys containing 2 at% of Nb, Ta or Mo. The glass containing tantalum exhibited the best corrosion properties since its active and passive current densities are nearly an order of magnitude lower than those for the other two alloys, see Fig. 12. All three of the alloys displayed secondary passivation at 1.5 V and showed similar E_{corr} values. The Nb-containing alloy had a somewhat lower passivating current density but a higher active current density than the Mo-containing alloy (Fig. 12).

The effect of different acid strengths (0.1 and 1.0 N H_2SO_4) and different potential scan rates (0.6 to 6.0 V h^{-1}) on the potentiodynamic polarization of $Fe_{59.4}Ni_{15.6}Cr_3Ta_2Si_8B_{12}$ alloy is given

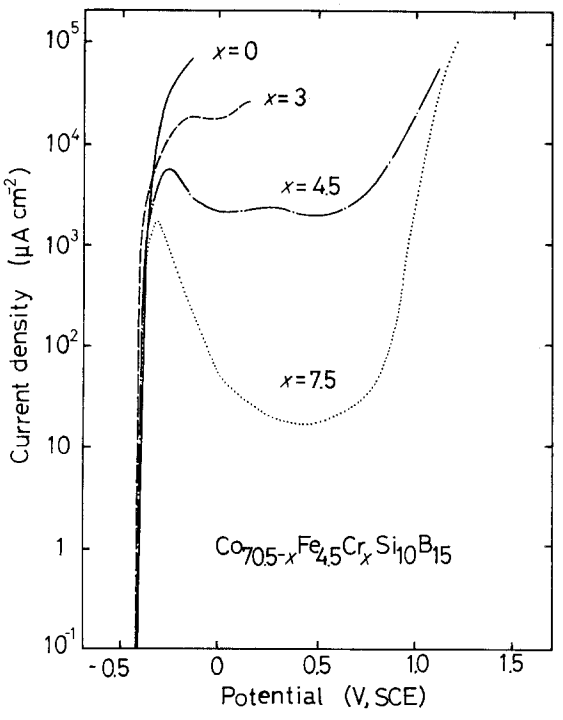

Figure 11 Effect of Cr-content on the potentiodynamic polarization curves of amorphous Co–Fe–Si–B alloys in 1.0 N H_2SO_4 with a potential scan rate of 0.6 V h^{-1}. Curves shown for $Co_{70.5-x}Fe_{4.5}Cr_xSi_{10}B_{15}$ where $x = 0$, 3, 4.5 and 7.5 [13].

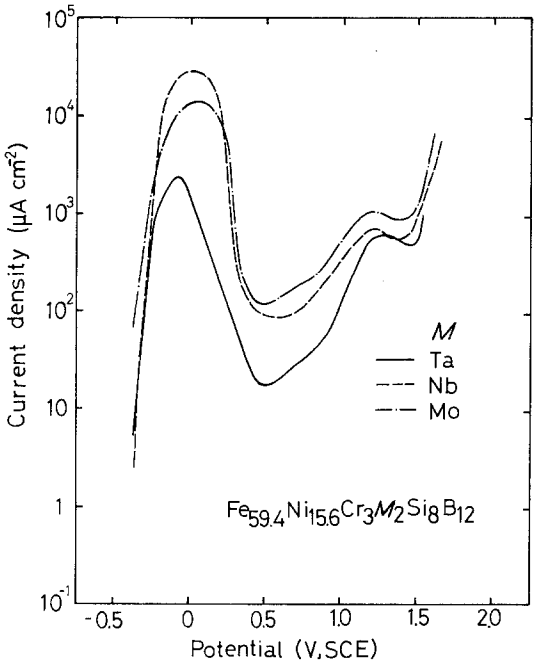

Figure 12 Potentiodynamic polarization curves of amorphous $Fe_{59.4}Ni_{15.6}Cr_3(Nb, Ta, or Mo)_2Si_8B_{12}$ alloys in 0.1 N H_2SO_4 at a potential scan rate of 6.0 V h^{-1} [13].

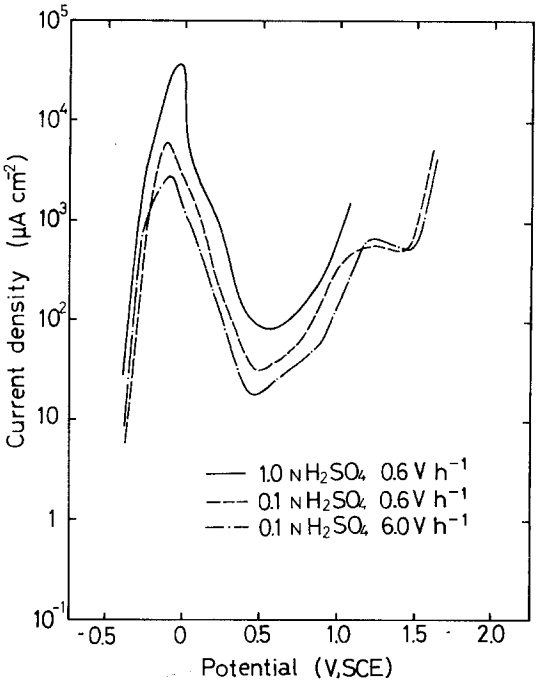

Figure 13 Potentiodynamic polarization curves of amorphous $Fe_{59.4}Ni_{15.6}Cr_3Ta_2Si_8B_{12}$ alloy in 0.1 N and 1.0 N H_2SO_4 at potential scan rates of 0.6 and 6.0 V h^{-1} [13].

in Fig. 13. The complete polarization curve was obtained for this alloy in all the tests shown here. However, the following points are noteworthy. In the case of Nb-containing alloy the samples severely corroded, in either 0.1 or 1.0 N H_2SO_4 in the active region before passivation occurred, at the slow potential scan rate of 0.6 V h^{-1}. The Mo-containing alloy gave a high rate of chemical attack in the active region and no passivation occurred in 1.0 N H_2SO_4; passivation did, however, take place in 0.1 N H_2SO_4, at a potential scan rate of 0.6 V h^{-1}.

Scanning electron microscopic studies of the $Fe_{59.4}Ni_{15.6}Cr_3Nb_2Si_8B_{12}$ alloy were also carried out through the different ranges of the polarization curve. Fig. 14a shows the rough "as-cast" surface before corrosion testing; Fig. 14b depicts the corroded surface after the sample failed in the active region when the potentiodynamic polarization experiment was conducted in 1.0 N H_2SO_4 at 0.6 V h^{-1}. When the sample was analysed using energy dispersive X-ray analysis (EDAX), the corroded surface in Fig. 14b was found to be rich in both Nb and Si. SEM photographs, shown in Fig. 15 were also obtained for this same Fe–Ni–Cr–Nb–Si–B alloy after potentiostatic tests in 0.1 N H_2SO_4 for 1 h, at 0.5 V in the passive region and at 1.75 V in the transpassive region. The

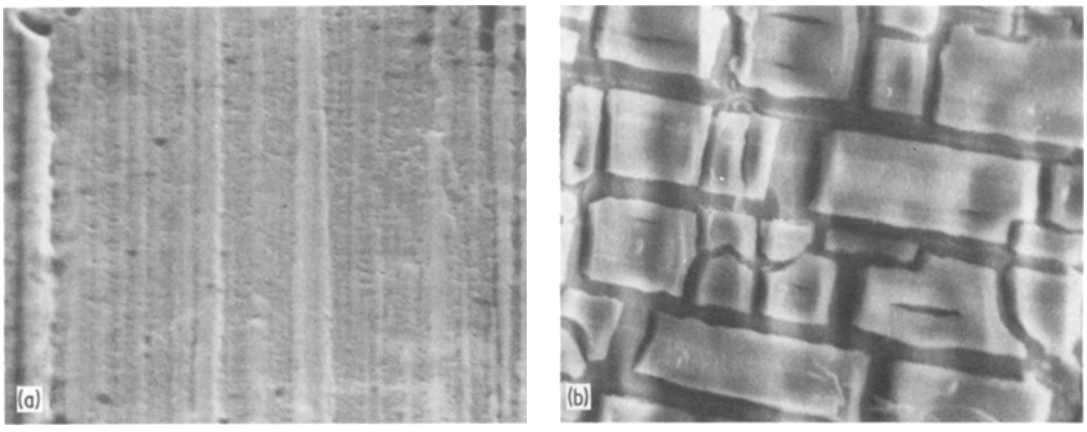

Figure 14 Scanning electron micrographs of amorphous $Fe_{59.4}Ni_{15.6}Cr_3Nb_2Si_8B_{12}$ alloy [13]. (a) "As-quenched" condition before corrosion test, × 2090; (b) after failure in the active region of a potentiodynamic polarization test in 1.0 N H_2SO_4 at a potential scan rate of 0.6 V h^{-1}, × 1100.

sample held in the passive region (Fig. 15a) showed very little change from the "as-cast" surface (Fig. 14a) except for the appearance of a river pattern on the surface. However, some pitting-corrosion attack is observed in the sample held in the transpassive region for 1 h in 0.1 N H_2SO_4 due to the higher potential (Fig. 15b). EDAX analysis of the corroded surface after failure in the transpassive region in 1.0 N H_2SO_4 at 6.0 V h^{-1} revealed enrichment of the Nb-content.

The following observations are evident from these current studies [7, 13] on the corrosion behaviour of iron-, cobalt- and nickel-base metallic glasses:

(a) Chromium, and nickel in the presence of chromium, are good alloying elements for the corrosion resistance of iron-base glasses;

(b) The Fe–Ni–B glasses have poor corrosion resistance properties in 2 N H_2SO_4 solution at 30° C, even in the case of the high Ni-content;

(c) Amorphous alloys of the type Fe–Si–B, Ni–Si–B and Co–Fe–Si–B have poor corrosion resistance in 0.1 and 1.0 N H_2SO_4 at 30° C and silicon contents up to 8 at % in the Fe- and Ni-base alloys and 10 at % in the Co-base alloy were insufficient to provide passivation;

(d) Chromium additions to the Co–Fe–Si–B glasses gave increased corrosion resistance to H_2SO_4 solutions; a Cr-content of 7.5 at % in the alloys resulted in a minimum passive current density, I_p, similar to that observed for the corrosion resistant alloy, $Fe_{70}Cr_{10}P_{13}C_7$, although the rate of formation of the passive film is slower for the Co-base alloy;

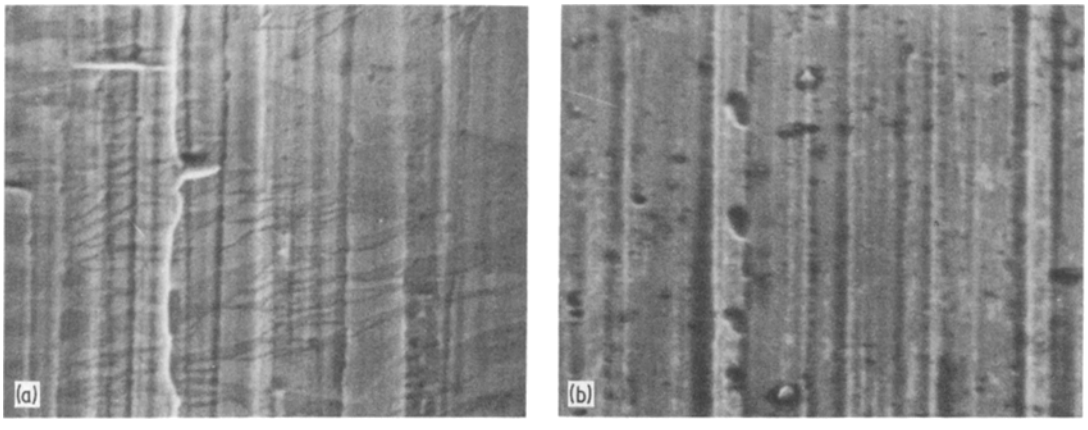

Figure 15 Scanning electron micrographs of amorphous $Fe_{59.4}Ni_{15.6}Cr_3Nb_2Si_8B_{12}$ alloy [13]. (a) Held at 0.5 V against SCE (passive region for 1 h at 0.1 N H_2SO_4, × 1975; (b) held at 1.75 V against SCE (transpassive region) for 1 h in 0.1 N H_2SO_4, × 985.

(e) Tantalum was a more effective alloying element for corrosion resistance in H_2SO_4 solutions than either niobium or molybdenum in $Fe_{59.4}Ni_{15.6}Cr_3(Nb, Ta \text{ or } Mo)_2Si_8B_{12}$ alloys;

(f) The chromium concentration appears to provide the most significant contribution to the corrosion resistance of the alloy glasses studied here;

(g) The corrosion resistance properties of metallic glasses may, in part, be due to their structural characteristics since they have no grain boundaries, segregates or crystalline defects that act as chemically active sites in crystalline metallic materials, but elemental composition is definitely a controlling factor in determining their corrosion behaviour.

4. Composition effect on the corrosion behaviour

Various proposals have been advanced to explain the higher corrosion resistance of metallic glasses compared with crystalline alloys of similar chemical composition. These proposals appear to depend on either the presence of specific alloying elements and/or the general structural characteristics of amorphous phase. The corrosion resistance of metallic glasses is partially related to the fact that there are no initiation sites for corrosion, such as grain boundaries and segregates. A uniform surface film is formed, which acts as a good passive film. The formation of this passive film is very rapid and, should a rupture of this film occur, a rapid recovery of the rupture also takes place. The glassy structure may be chemically more active than the crystalline one. This would, of course, be based on the actual composition of the alloy from which the amorphous phase is made. However, metallic glasses are characterized as chemically homogeneous, owing to their single-phase nature without the crystalline defects that normally act as chemically active sites in crystalline alloys. On the other hand, there are a large quantity of metalloid elements such as B, C, P and Si in the solid solution matrix and these additive elements should greatly affect the corrosion behaviour of the alloying glasses, again based on actual composition. Thus the compositional effect, in particular, should be considered to be one of the important factors in discussing the corrosion behaviour of metallic glasses.

Fig. 16 illustrates the compositional effect of alloying element, M, on the corrosion rates of the Fe–M–$P_{13}C_7$ glasses in 0.1 N HCl solution (Fig. 16a) and a 0.1 N H_2SO_4 solution (Fig. 16b), respectively [16]. The results of crystalline Fe–Cr alloys with different Cr contents are also given in Fig. 16a, for comparison. With the exception of manganese, the corrosion rate is decreased by

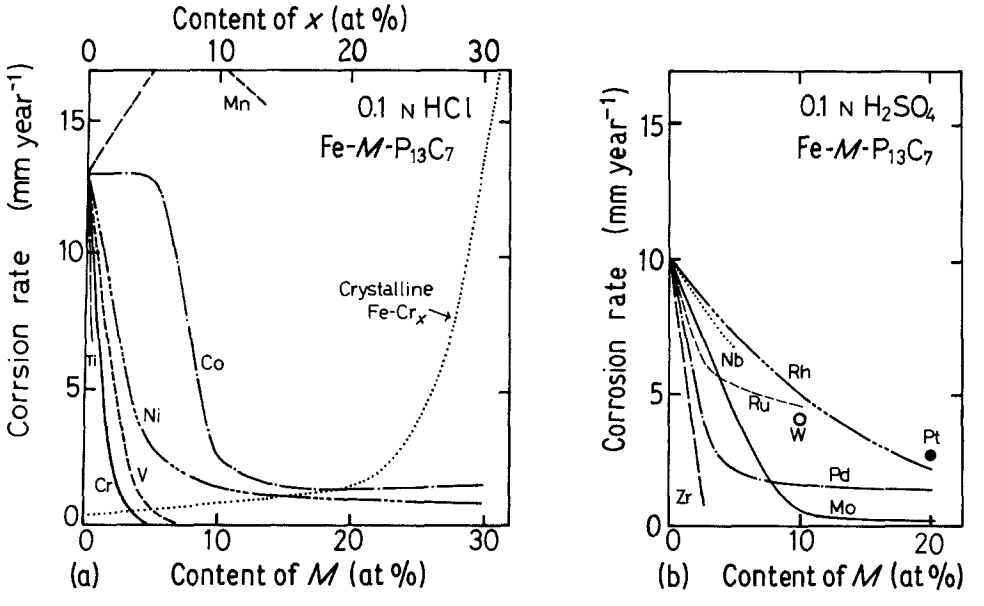

Figure 16 Variation of corrosion rates of glassy Fe–M–$P_{13}C_7$ as a function of content of alloying element, M. (a) In 0.1 N HCl solution at 30° C, where M is CR, V, Ni, Co or Mn; (b) in 0.1 N H_2SO_4 solution at 30° C, where M is Zr, Nb, Rh, Ru, Pt, W, Pd or Mo. A broken curve in (a) indicates the corrosion rate of crystalline Fe–Cr_x alloys in 0.1 N HCl solution at 30° C as a function of x [16].

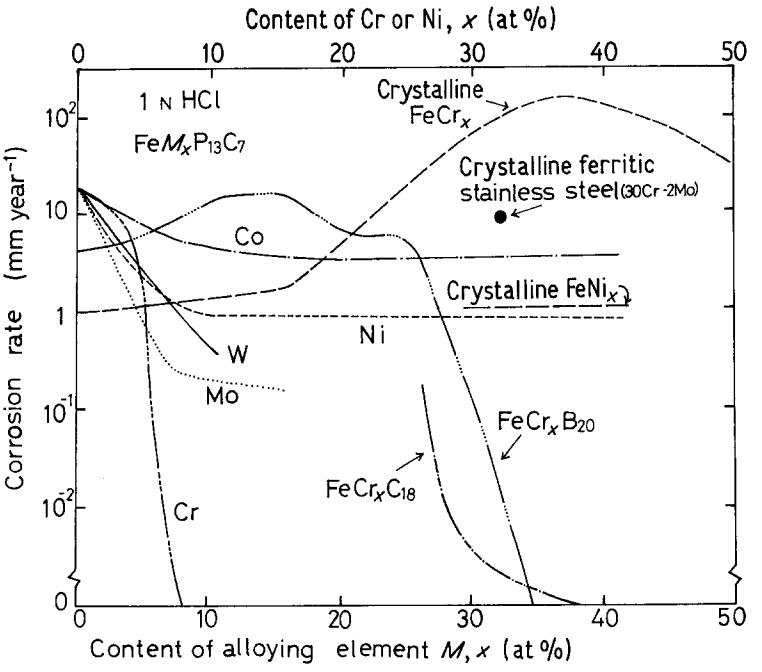

Figure 17 Changes in average corrosion rates of glassy Fe–*M*–13P–7C alloys in 1 N HCl at 30° C as a function of content of alloying element, *M*, where *M* is Cr, Mo, W, Ni or Co. Corrosion rates of various crystalline alloys as functions of Cr or Ni contents, *x*, are also shown for comparison [17].

alloying with almost all metallic elements as the second metallic elements of the glassy alloy. Additions of Zr, V, Nb, Mo or W, as well as Ti and Cr, are effective for improving corrosion resistance, as shown in Fig. 16. Here, all these elements are more active than the main constituent element of Fe. The addition of elements more noble than main constituent element of the alloy is also effective. Fig. 17 gives the change in corrosion rate of the Fe–*M*–$P_{13}C_7$ glasses in a 1 N HCl solution as a function of content of alloying element of *M* [17]. The addition of Cr is again found to be most effective in improving the corrosion resistance producing spontaneous passivation in the glasses containing 8 at % or more Cr. The addition of Mo follows the Cr effect for improvement of the corrosion resistance of Fe–P–C-type glasses. It is also noticed that the addition of a small amount of Mo (about 5 at %) leads to a greater decrease in corrosion rate than the addition of an equivalent amount of Cr; the addition of Co is not as effective in improving the corrosion resistance of the Fe–P–C-type glasses in 1 N HCl solution.

The effects of additive elements in improving corrosion resistance are especially significant when a small amount of Cr exists in the Fe–P–C-type glasses [14]. This suggests that the extra metallic elements interact co-operatively with the Cr. Studies have been carried out showing the change in corrosion rates of the glasses of Fe–$Cr_3P_{13}C_7$–*M*, where *M* is the extra metallic element. Fig. 18 shows the results of some of these studies, where *M* is Ti, Mn, Nb, V, W or Mo in a 1 N HCl solution at 30° C, as a function of extra metallic elements [14]. Additions of Mo, W, Ti and V are particularly effective in rapidly decreasing the corrosion rate. Fig. 19 gives the potentiodynamic polarization curves of the Fe–$Cr_3P_{13}C_7M_2$ glasses [14]. The glass with no extra alloying element is unstable in 1 N HCl solution and hence a complete anodic polarization curve was not obtained. By the

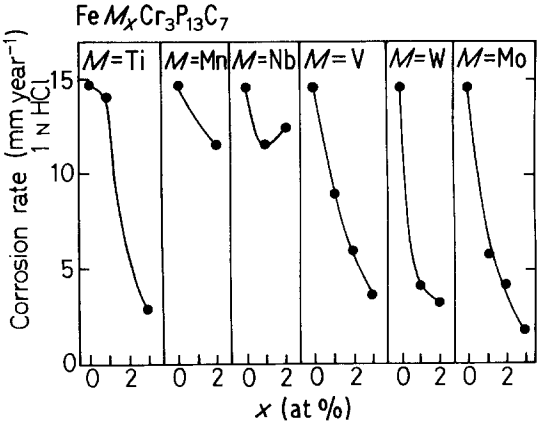

Figure 18 Variation of average corrosion rates estimated from the weight losses by addition of different amounts of various metallic alloying elements to amorphous Fe–3Cr–13P–7C alloy in a 1 N HCl solution at 30° C [14].

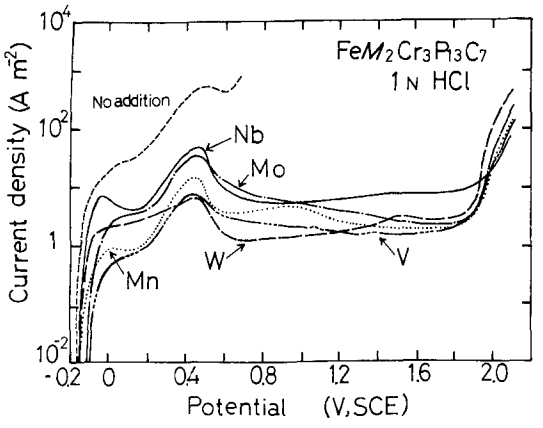

Figure 19 Anodic polarization curves produced by additions of various extra metallic alloying elements, M, in amorphous Fe–3Cr–13P–7C–2M alloys exposed to a 1 N HCl solution, where M is Nb, Mo, Mn, W or V [14].

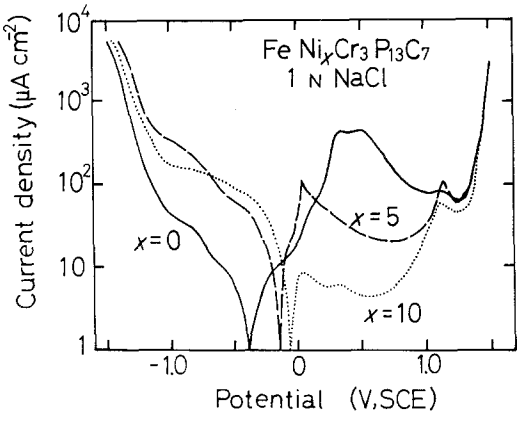

Figure 20 Potentiodynamic polarization curves of amorphous Fe–3Cr–xNi–13P–7C alloys measured in a 1 N NaCl solution. Curves are shown for Ni-contents (at%), x, of 0, 5 and 10 [19].

addition of an extra alloying element of 2 at%, the measurement of nearly complete polarization curves of metallic glasses containing only 3 at% Cr becomes feasible as far as the region of oxygen evolution, without showing an abrupt rise in current due to pitting corrosion, even in 1 N HCl solution. This is a most interesting characteristic of metallic glasses. According to Sugimoto and Sawada [18], in order to measure anodic polarization curves for crystalline stainless steel in 1 N HCl solution up to the region of the transpassive reaction of Cr (which is within a few hundred mV of the oxygen evolution potential) ferritic stainless steels must contain at least 30 at% Cr.

Of greater interest, are the results showing that the addition of Ni appreciably improves the corrosion resistance of metallic glasses with a small amount of Cr [19]. As shown in Fig. 20, the Fe–$Cr_3P_{13}C_7$ glass has a fairly high corrosion resistance in 1 N HCl solution [19]. The current density in the passive region is shown to decrease significantly upon the addition of Ni to this metallic glass. The active region almost disappears in the glass of Fe–$Cr_3Ni_{10}P_{13}C_7$. These studies have shown that Ni addition to the Cr-bearing iron-base metallic glasses does not constitute a passive film but promotes the formation of a passive film which is mainly composed of hydrated chromium oxyhydroxides [9]. In other words, the Ni addition interacts co-operatively with the Cr. Therefore, the decrease of the anodic current density of the Fe–Cr_3–Ni–$P_{13}C_7$ glasses in the passive region, caused by an increase of the Ni-content, can be attributed to the promotion of passive film formation, that is, the increase in the formation rate of the passive film and the improvement of uniformity of the passive film which lowers the dissolution rate of the alloys. These results clearly imply that the addition of small amount of extra metallic elements remarkably enhances the corrosion resistance of Fe–$Cr_3P_{13}C_7$-type glasses.

Metalloid elements such as B, C, P and Si are necessary structural components of metallic glasses and play a significant role in their amorphous phase formation. This is especially true for the formation of amorphous phase in Fe-, Cr- and Ni-base alloys by rapid quenching from the melt. These additive metalloid elements should affect the corrosion behaviour of metallic glasses [10, 20]. The effects of a metalloid, X, on the corrosion rate of the Fe–$Cr_{10}P_{13}X_7$-type and Fe–$Cr_{10}B_{13}X_7$-type glasses in 0.1 N H_2SO_4 solution at 30° C are given in Fig. 21 [20]. It is obvious from this particular study that the corrosion rates of metallic glasses containing P as a major metalloid addition are more than two orders of magnitude lower than those of the alloy glasses containing B as a major metalloid addition. It is also shown that the corrosion rate in 0.1 N H_2SO_4 solution of the Fe–Cr-type glasses is progressively decreased in the order: Si, B, C and P. In other words, the addition of Cr with Si, B or C to iron-base metallic glasses is not so effective in improving their corrosion resistance properties as the addition of Cr with P, as seen in the results of Fe–Cr–$B_{13}C_7$ and Fe–Cr–$B_{13}Si_7$ glasses [10]. Fig. 22 shows the effects of minor additions of metalloids, X, on the reactivity of the bare Fe–$Cr_{10}B_{13}X_7$ glasses

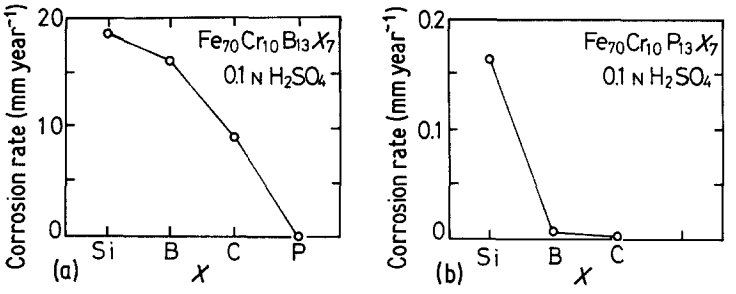

Figure 21 Average corrosion rates estimated from the weight loss of amorphous Fe–10Cr–13B–7X and Fe–10Cr–13P–7X alloys in 0.1 N H_2SO_4 at 30° C, where (a) X is Si, B, C and P and (b) X is Si, B and C [20].

after mechanical abrasion of the specimen surfaces during potentiostatic polarization tests in the passive region [21]. The extrapolations given by the dotted lines in Fig. 22 correspond to the expected values of the reactivities of the glasses. A sharp decrease in current density with time corresponds to the rapid decrease in reactivity of the bare surface, that is, the rapid formation of a passive film. The P-bearing alloy glass exhibits the highest current density immediately after mechanical abrasion, corresponding to the highest reactivity of the alloy glass itself, and shows the lowest steady current density related to the highest protective quality of the passive film. Thus, it is evident that phosphorus is the most effective metalloid element for improving the corrosion resistance properties of iron-base metallic glasses containing a certain amount of Cr. This is also confirmed by the results of Fig. 17 [6]. The effect of Cr is most remarkable in the case of Fe–Cr–$P_{13}C_7$ glass, while addition of Cr to the Fe–C-type and Fe–B-type glasses is ineffective below about 20 at %. However, the corrosion rates of the Fe–$Cr_{26}C_{18}$ and Fe–$Cr_{30}B_{20}$ glasses are nearly two orders of magnitude lower than that of the 30Cr–2Mo-type crystalline stainless steel. Furthermore, the addition of Cr to these glasses leads to immunity to corrosion by spontaneous passivation even in 1 N HCl solution open to the air. On the other hand, the 30Cr–2Mo-type ferritic stainless steel remains in the active region.

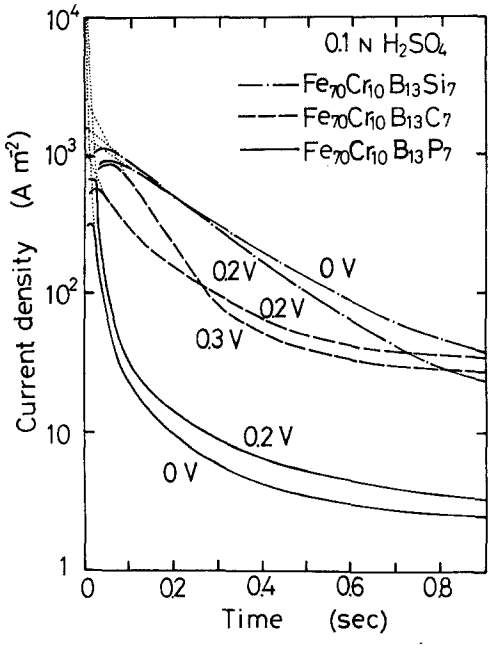

Figure 22 Current density–time curves of amorphous Fe–10Cr–13B–7X alloys immediately after mechanical abrasion of specimen surfaces during anodic polarization at constant potentials in 0.1 N H_2SO_4, where the minor metalloid, x, is Si, C or P. The polarization potentials relative to the saturated calomel electrode are also shown [32].

Similar results have been reported from the results of electrochemical measurements [22]. These studies showed that, in general, the lower the peak current density in the active region and the higher the corrosion potential, the lower is the corrosion rate. Specifically, as shown in Fig. 23, the peak current densities of the Fe–$Cr_{10}B_{20}$, Fe–$Cr_{10}B_{13}Si_7$ and Fe–$Cr_{10}B_{13}C_7$ glasses in the active region are one order of magnitude higher than that of the Fe–$Cr_{10}B_{13}P_7$ glass, and the

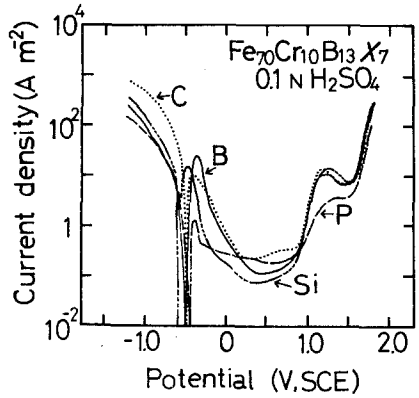

Figure 23 Potentiodynamic polarization curves of amorphous Fe–10Cr–13B–7X alloys in 0.1 N H_2SO_4 for metalloid, x, where x is C, B, Si or P [21].

TABLE III Results of XPS analysis of film found on amorphous Fe–10Cr–13P–7C alloy before and after immersion in 1 N HCl at 30° C for 168 h [9]

History	Cationic fraction in film			$Fe^{II}/(Fe^{II} + Fe^{III})$ ratio	O^{2-}/total O ratio
	Cr	Fe	P		
Before immersion	0.65	0.32	0.02	0.25	0.40
After immersion	0.95	0.03	0.02	0.41	0.50

corrosion potentials are raised progressively by the addition of 7 at% of Si, B, C and P. It was noticed again that a significant increase in the corrosion resistance of iron-base metallic glasses by the addition of Cr cannot be attained unless phosphorus exists as a major metalloid element addition. These results also indicate that the combination of metalloids which produces superior corrosion resistance in the Fe–Cr-type glasses is phosphorus and/or carbon. The importance of the addition of P in improving the corrosion behaviour has also been observed [22] in glasses of metal–metal-type, which are composed of two metallic elements such as Cu–Zr. Such information will be given in Section 6.

5. Passive film formation

The high corrosion resistance of metallic glasses containing Cr and P is attributable to the rapid formation of a passive film with a high protective quality and a high uniformity. The composition of the passive film formed on crystalline Fe–Cr alloys, determined by using X-ray photoelectron spectroscopic analysis, depends on the Cr content in the alloys [23]. In general, the corrosion resistance of the alloys containing a certain amount of Cr is partly dependent upon the concentration of trivalent Cr in the surface films. Metallic glasses are not exceptional in this characteristic. Results of X-ray photoelectron spectroscopic analysis of surface films formed on the $Fe–Cr_{10}P_{13}C_7$ glass in 1 N HCl solution are summarized in Table III [24]. The passive film formed on this alloy consists exclusively of hydrated chromium oxyhydroxide, $CrO_x(OH)_{3-2x} \cdot nH_2O$, and shows a high protective quality. This composition is not essentially different from that of the passive films formed on the crystalline Fe–Cr alloys [23]. However, the concentration of hydrated chromium oxyhydroxide in the passive films and the values of n and x are different for the amorphous phase and the crystalline phase stainless steel, depending on the composition of the desired alloy and the condition of the film formation. The passive film consists of hydrated iron oxyhydroxide unless Cr is contained in iron-base glasses. If the Cr-content of the passive film is increased the stability of the film is greater. The passive film formed on the metallic glasses contains a significant enrichment of hydrated chromium oxyhydroxide in comparison with that formed on crystalline high Cr-content alloys, such as ferritic stainless steel containing 30 at% Cr, as shown in Table IV. The concentrations of H_2O and OH in the passive films on various metallic glasses are also higher than those found in the films on the crystalline stainless steels. The presence of H_2O and OH in the film produces the following effects on the corrosion resistance [25]: (a) H_2O and OH act as the effective species to capture the dissolving metal ions and consequently assist in the formation of new protective film against a further attack by the corrosive environment; (b) H_2O and OH are also able to form a cross-linked monolithic amorphous passive film without grain boundaries, producing increased film ductility discouraging mechanical breakdown of the film. The formation of a passive film with such a high protective quality results in a higher corrosion resistance than is possible for the crystalline stainless steel, even though the Cr-content of metallic glasses is considerably lower.

TABLE IV Chromium contents of passive films formed on alloy glasses and crystalline stainless steel in 1 N HCl solutions

Sample	Cr^{III}/total metallic ions ratio*	Passivation method	Reference
Alloy glasses			
$Fe_{70}Cr_{10}P_{13}C_7$	0.97	spontaneous	[9]
$Ni_{71}Cr_9P_{15}B_5$	0.74	spontaneous	[5]
$Co_{70}Cr_{10}P_{20}$	0.95	spontaneous	[22]
Ferritic stainless steel			
Fe–30Cr	0.75	polarization	[37]
Fe–19Cr	0.58	polarization	[38]

*When passivation occurs by anodic polarization, the table shows the maximum value of cationic fraction of chromium in the passive film.

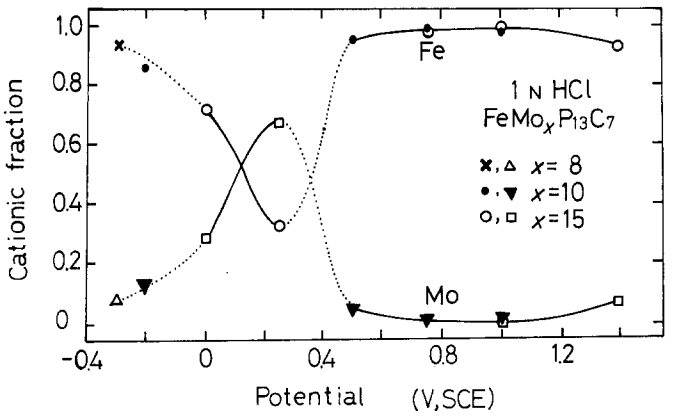

Figure 24 XPS results of changes in cationic fractions of molybdenum and iron in surface films formed on amorphous Fe–Mo–13P–7C alloys by polarization for 1 h at various constant potentials in a 1 N HCl solution [26].

As discussed in the previous section, the addition of metallic elements to metallic glasses results in an improvement of the corrosion resistance. This alloying effect may be partly interpreted as the enrichment of these additive elements in the surface films. As shown in Fig. 24 [26], the active elements such as Mo, rather than the main constituent of Fe in iron-base glasses, are highly concentrated in the surface films formed in the active region of alloys; the faster the active dissolution, the higher is the concentration of the active element (e.g., Mo) in the surface films. This implies that active dissolution of alloys containing one or more of these elements gives rise to the formation of corrosion product films in which these elements are highly concentrated. The enrichment of these additive elements in the corrosion product films improves the protective quality of the films which act in turn as a diffusion barrier to the dissolution of alloys, thus decreasing the corrosion rate.

A high degree of chemical homogeneity is another characteristic of metallic glasses. An examination of the effect of alloy homogeneity on corrosion behaviour, and not the effect of crystallinity, has been carried out [11]; the influence on corrosion of crystallinity, *per se*, would require a comparison of an amorphous alloy and a perfect single-crystal of the crystalline alloy with the same chemical composition. The Fe–$Cr_{10}P_{13}C_7$ glass was selected and, by careful heat treatment at 350° C for 2 months in an evacuated quartz capsule, the alloy was crystallized into a single b c c-phase with grains of 5 to 10 nm diameter. The potentiostatic polarization curves of the crystalline alloy could not be obtained, due to the rapid disappearance of the specimen by anodic dissolution during polarization in 1 M H_2SO_4 solution [11]. As shown in Fig. 25, the comparison of the crystallized alloy with the amorphous phase having the same composition was performed by means of potentiodynamic polarization measurements. The results show that the anodic current density of the crystallized alloy of Fe–$Cr_{10}P_{13}C_7$ is more than two orders of magnitude higher than that of the glass with the same composition.

Scanning electron micrographs of the crystallized alloy after immersion in 1 N H_2SO_4 solution for 15 min reveal uneven, severe general corrosion [11]. This high reactivity results from a high density of localized crystal defects, such as grain boundaries and segregates. It follows that the extremely high corrosion resistance of certain metallic glasses results partly from the formation of a uniform passive film, since the underlying, completely homogeneous, single-phase alloys are without localized crystalline defects that can act as nucleation sites for corrosion. In other words,

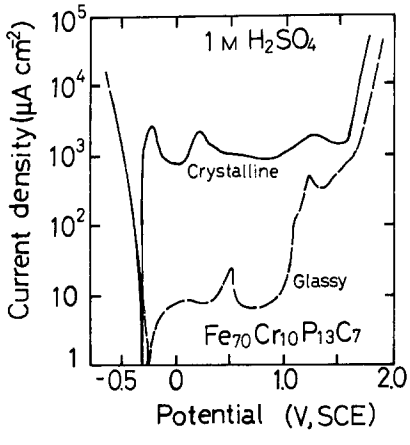

Figure 25 Potentiodynamic polarization curves of amorphous and crystallized Fe–10Cr–13P–7C alloys measured in 1 M H_2SO_4. The crystallized alloy consisted of a single b c c phase with fine grains of diameters in the range 5 to 10 nm [11].

the protective quality of the passive film is determined not only by the composition of the film but also by the degree of chemical homogeneity and single-phase nature of the metallic glasses. Such single-phase nature will again be discussed for the Ti–Ni alloys in Section 6.

The corrosion resistance of metallic glasses depends on the rate of passive film formation as well as on the degree of homogeneity of the passive films. The passivation of metals generally occurs through the active dissolution of metals during the initial time period; an increase in the concentration of soluble elements or hydroxyl ions in the vicinity of the electrode surface occurs, that is, active dissolution is necessary for the subsequent passive film formation by precipitation or anodic deposition. In addition, the high corrosion resistance is partly a result of the high rate of passivation which takes place when the passive film breaks down, either mechanically or chemically. In order to compare the formation rates of passive films on metallic glasses with those on stainless steels, an investigation was carried out wherein the change in current density with time was measured after abrading the specimen surface during anodic polarization at various constant potentials in the passive region [11]. Fig. 26 shows the change in the current density immediately after film removal by abrading the specimen surface in the solution during anodic polarization. The current density of the $Fe–Cr_{10}P_{13}C_7$ glass immediately after abrasion (time = 0 in Fig. 26) is higher than that of the conventional 18-8 stainless steel, indicating that a metallic glass without surface films is more reactive than the conventional stainless steels. As is also indicated in Fig. 26, the metallic glass exhibits a higher rate of current density decrease after cessation of abrasion. This sharp decrease in current density with time corresponds to the rapid decrease in the reactivity of the bare specimen surface caused by the rapid formation of the protective film. As shown in Fig. 26, regarding the measurements taken in 1 M H_2SO_4 plus 0.5 N NaCl solution, the current decay of the glass after film removal is not significantly affected by the addition of Cl-ions into the solution. The high reactivity of metallic glasses facilitates the enrichment of trivalent Cr at the bulk material–solution interface and leads to the rapid formation of a passive film consisting of hydrated chromium oxyhydroxide. This partly accounts for the extremely high corrosion resistance of metallic glasses.

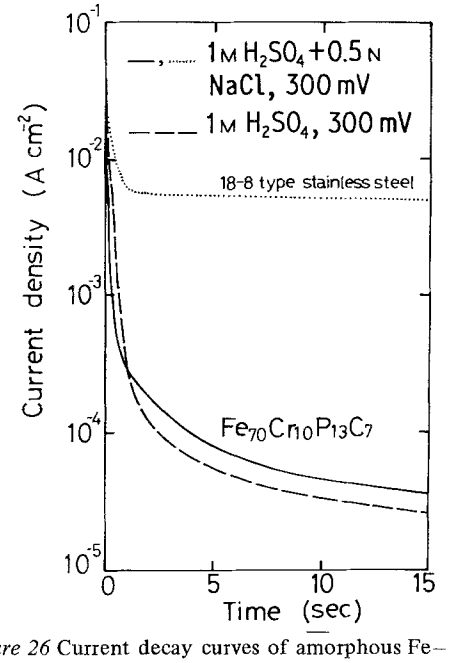

Figure 26 Current decay curves of amorphous Fe–10Cr–13P–7C alloys and 18Cr–8Ni stainless steel after the cessation of abrasion (at time = 0) during polarization at + 300 mV (SCE) [20].

6. On the corrosion behaviour of metal–metal-type glasses

Glass-forming alloys generally include one or more kind of metalloid elements, such as B, C, P and Si, in their constituents. However, the corrosion behaviour of alloy glasses of the metal–metal-type is also of great interest. Such work was carried out, by Naka *et al.* [22], on the corrosion characteristics of $Cu_{50}Zr_{50}$ and $Cu_{50}Ti_{50}$ alloy glasses compared with those of the crystallized alloys and pure elements of Cu, Zr and Ti in varous solutions. Their results clearly demonstrate that the corrosion resistance of these alloys is definitely higher than that of the crystallized alloys having the same composition, as shown in Fig. 27. However, the corrosion behaviour of metal–metal-type glasses without metalloid elements mainly depends on the content of the constituent elements having the higher corrosion resistance.

The Fe–Si glasses may be classified as of the metal–metal-type from the corrosion point of view from the following experimental data. Brusic *et al.* [27] reported the corrosion behaviour of Fe–Si glasses produced by a sputtering technique. According to their results, the corrosion rate in a dilute sulphuric acid solution decreases by a factor of 50, when the Si-content increases from

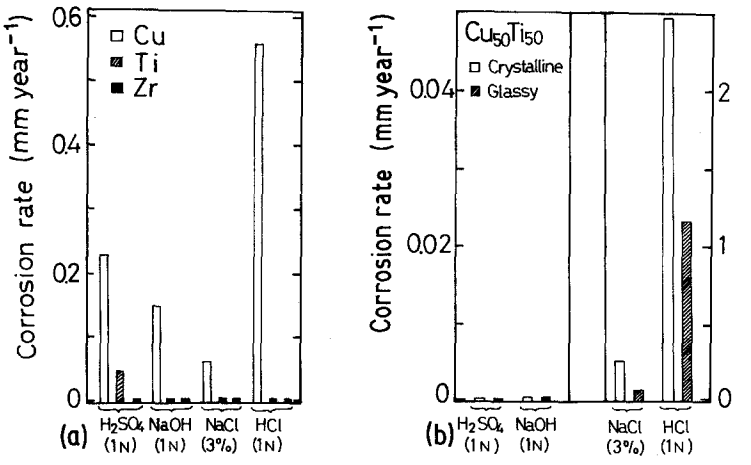

Figure 27 Average corrosion rates estimated from the weight loss of pure Cu, Ti, Zr and $Cu_{50}Ti_{50}$ in 1 N H_2SO_4, 1 N NaOH, 3 at% NaCl and 1 N HCl solutions at 30° C [21].

20 to 30 at% even in the crystalline state. This is mainly due to passivation by silicon. Thus the $Fe_{70}Si_{30}$ glass shows a corrosion rate only about one order of magnitude lower than that of the crystalline $Fe_{70}Si_{30}$. This experimental result implies that the amorphous phase formation is definitely effective in improving the corrosion resistance; however, the dominant factor for the corrosion behaviour of Fe–Si alloys is their silicon content. A similar behaviour regarding the passivation by silicon has also been reported in a corrosion study of Pd–Si glass [28].

Based on these experimental observations, an extremely high corrosion resistance, as observed for the metal–metalloid-type glasses such as $Fe–Cr_{10}P_{13}C_7$, could not be expected for alloy glasses of metal–metal-type containing no metalloid elements. However, the addition of a small quantity of a metalloid, such as P, to the metal–metal-type glasses remarkably improves their corrosion resistance, as exemplified by the results from a study of Cu–Ti glass shown in Fig. 28 [22]. The corrosion resistance of $Cu_{50}Ti_{50}$ glass is lower than that of crystalline pure titanium due to the detrimental effect of Cu. As shown in Fig. 28 [22], the $Cu_{50}Ti_{50}$ glass shows a high current density in both the active and passive region in 1 N HCl solution. Even if the Ti-content is raised to 70 at%, the corrosion potential of the glass is still lower than that of crystalline titanium. However, the corrosion resistance becomes higher than that of the crystalline titanium in relation to spontaneous passivation when 5 at% P is added to this alloy glass. Particularly, the passive current density of the $Cu_{25}Ti_{70}P_5$ glass, measured in 1 N HCl solution, is about two orders of magnitude lower than that of crystalline titanium as shown in Fig. 24. This fact may be interpreted in terms of the rapid formation of a Ti-concentrated passive film due to the acceleration of active dissolution by P.

It is now well-accepted that the solid solution of a single phase, not amorphous phase, can be obtained by rapid quenching from the melt. This results in homogeneous alloys, rather than the multiphase crystalline state produced by slow cooling, and may contribute partially to the improved corrosion resistance of metallic materials. Such behaviour has recently been reported from the study of rapidly-quenched crystalline Ti–Ni

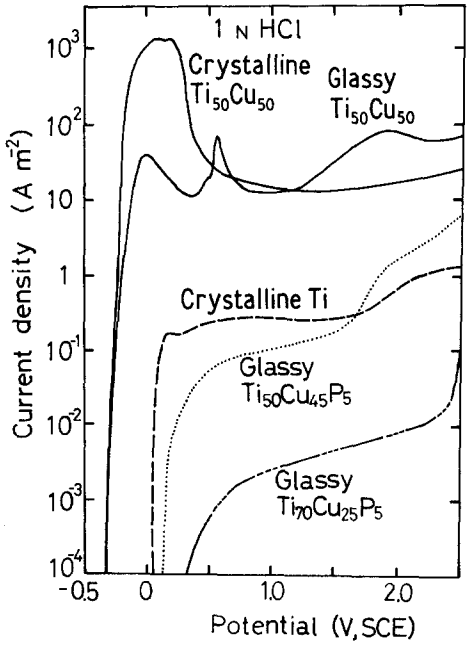

Figure 28 Anodic polarization curves of amorphous and crystalline Ti–Cu alloys and amorphous Ti–Cu–P alloys measured in a 1 N HCl solution [21].

alloys [29]. The usual crystalline alloys, having 40 and 61.6 at % Ni, consist of multiphase mixtures such as Ti_2Ni, TiNi, etc. Both rapidly-quenched $Ti_{60}Ni_{40}$ and $Ti_{38.5}Ni_{61.5}$ alloys are composed of a single TiNi-type phase with a fine-grain structure indicating an expansion of the homogeneous range of the compound as a result of rapid-quenching. As shown in Fig. 29, the crystalline multiphase alloys exhibit high anodic current densities in 1 N HCl solution and indicate little tendency to passivate by anodic polarization. Contrary to this result, the rapidly-quenched crystalline single-phase alloys reveal significantly lower anodic current densities, particularly the rapid-quenched crystalline $Ti_{60}Ni_{40}$ alloy having a single phase which passivates spontaneously and shows a lower passive current density than that of pure crystalline titanium. The formation of amorphous phase by adding a small amount of phosphorus is further effective in improving the corrosion resistance, as seen from a comparison of the polarization curves of the three different states of Ni–Ti-base alloys containing 38.5 at % Ti: crystalline $Ti_{38.5}Ni_{61.5}$, rapidly-quenched crystalline $Ti_{38.5}Ni_{61.5}$ and glassy $Ti_{38.5}Ni_{56.5}P_5$. A similar approach due to single-phase formation by rapid quenching from the melt may be another way, as well as the addition of a small amount of P as an alloying element, to improve the corrosion resistance behaviour of some crystalline metallic materials [30].

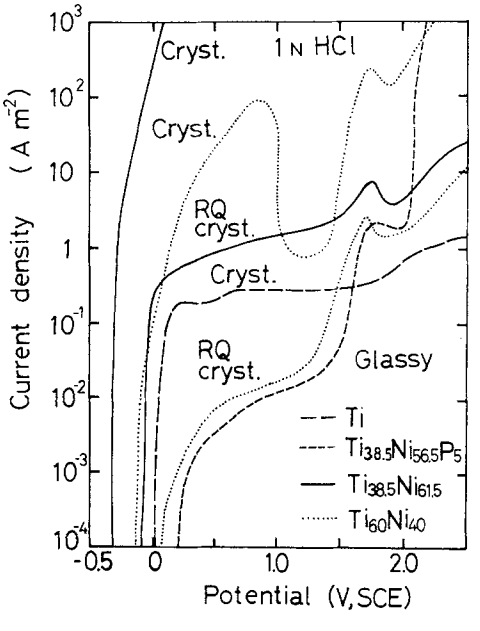

Figure 29 Anodic polarization curves of ordinary crystalline Ti–Ni alloys, rapidly-quenched (RQ) crystalline Ti–Ni alloys and amorphous Ti–Ni–P alloy, measured in 1 N HCl solutions [29].

7. Stress corrosion cracking

Various metallic glasses, especially those of the metal–metalloid-type, show excellent corrosion resistance as well as good mechanical and magnetic properties. The excellent corrosion resistance of metallic glasses to pitting corrosion may be interpreted in terms of their resistance to pit nucleation which can be attributed both to their high degree of chemical homogeneity and to their lack of inclusions resulting from being rapidly quenched.

However, the production of metallic glasses is not always the answer to the problem of corrosion resistance. For example, Davine [31] has reported that $Ni_{55}Fe_{20}Cr_5P_{14}B_6$ glass is sensitive to crevice corrosion after the glass was cold-rolled. In this case, severe cold-rolling induced some cracks in the bulk materials and crevice corrosion then occured at these cracks. It was also found that plastic deformation has no influence on either passive corrosion current density or pitting corrosion resistance; the mechanism of deformation in metallic glasses is not fully understood as yet, although it is known that the metallic glass case differs from the crystalline alloy case in this regard [32]. For these reasons, the susceptibility of metallic glasses to stress corrosion cracking is of considerable interest. The available information is given below.

Kawashima *et al.* [33] studied the stress corrosion cracking behaviour of Fe–$Cr_{7.5}Ni_{23}P_{13}C_7$ glass subjected to constant strain rates at room temperature in an H_2SO_4 acid solution containing Cl^- ions. Fig. 30 shows typical tensile stress–strain curves measured at room temperature in air and in solution [33]. The fracture stresses at anodic, cathodic and corrosion potentials E_+, E_- and E_{corr}, respectively, in 5 N H_2SO_4 + 0.1 N NaCl solution are lower than that in air. The cathodic polarization (Curve 4) gives the largest decrease in fracture stress. According to the scanning electron microscopic study [34], the fracture surface in air shows a smooth region produced by large local plastic shearing and a vein-like region formed by plastic instability. This corresponds to typical features with respect to the morphology of the fracture surface in metallic glasses [32]. The fracture surface produced during cathodic polarization gives the typical brittle pattern character-

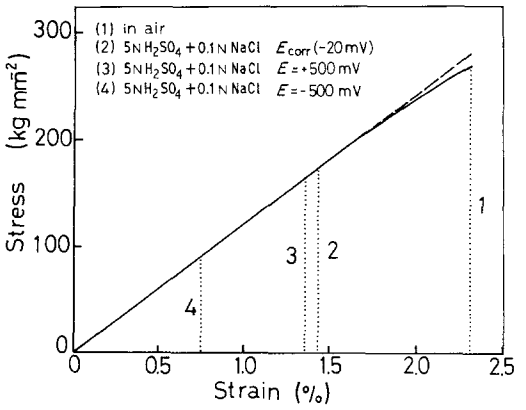

Figure 30 Stress–strain curves of amorphous Fe–7.5Cr–23Ni–13P7C alloy, in air and in solutions at various potentials, at a strain-rate of 4.2×10^{-6} sec^{-1} [33].

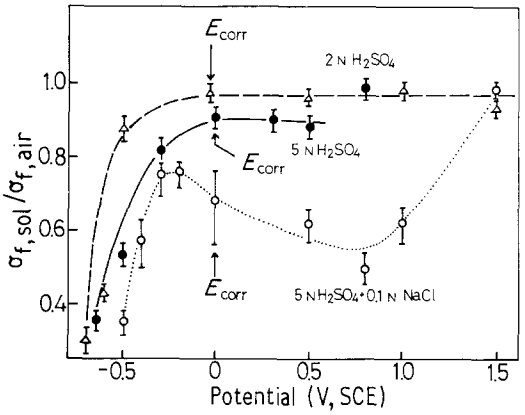

Figure 32 Variation of susceptibility to cracking of amorphous Fe–7.5Cr–23Ni–13P–7C alloy as a function of applied potential in 2 N and 5 N H_2SO_4, and in 5 N H_2SO_4 + 0.1 N NaCl solutions at a strain-rate of 5.6×10^{-6} sec^{-1} [33].

ized by a granular structure. As shown in Fig. 31 [35], the fracture stress decreases only when the tensile stress was applied to the glassy samples in relatively strong acidic solutions containing a certain concentration of Cl^{-1} ions. However, no embrittlement is observed during tests in neutral NaCl solutions and in acidic solution with low Cl^{-1} ion concentration.

Fig. 32 gives the change in the susceptibility to cracking of the Fe–$Cr_{7.5}Ni_{23}P_{13}C_7$ glass as a function of the applied potential in 2N and 5N H_2SO_4 solutions and in a 5 N H_2SO_4 + 0.1 N NaCl solution. The susceptibility to cracking is quantified by the ratio of the fracture stress in solution, $\sigma_{f\,sol}$, to that in air, $\sigma_{f\,air}$ [33]. In the potential region less noble than the hydrogen evolution potential, the stress corrosion cracking susceptibility increases with decreasing potential in solutions both with and without Cl^{-1} ions. This observation is attributed to hydrogen embrittlement. However, the fracture stresses measured in 2N and 5N H_2SO_4 solutions in the higher potential region are similar to that measured in air. The fracture stress in the passive region, including the corrosion potential in the 5N H_2SO_4 + 0.1 N NaCl solution, appears to decrease as the potential increases. The glass corrodes when the transpassive reaction occurs and then the fracture stress is the same order of magnitude as that obtained in air. These results suggest that the metallic glass is not subjected to stress corrosion cracking in the solutions and at potentials presently investigated [33]. The fracture behaviour of metallic glasses observed during tests in solutions under stress is considered to be due to hydrogen embrittlement. This result is also confirmed by the following experiments. Fig. 33 gives the stress–elongation curves of Fe–$Cr_7Ni_{20}P_{14}C_6$ glass under various cathodic polarization conditions [34]. The fracture stress of the hydrogenized sample (Curve 1) is considerably less than that in air. However, such a sample shows an increase in fracture stress after exposure to air for 1 h, as exemplified by Curve 2. The fracture stress obtained for a hydrogenized sample in oil at 100° C or in vacuum (Curve 3) is very similar to the value obtained in air. Curves 4 and 5 suggest that cathodic polarization does not affect the fracture stress during traction in liquid nitrogen. As shown in Table V [34], the amount of hydrogen absorbed during cathodic polarization at −500 mV is one order of magnitude higher than that for the as-quenched sample. Therefore, the embrittlement of metallic glass subjected to cathodic polarization

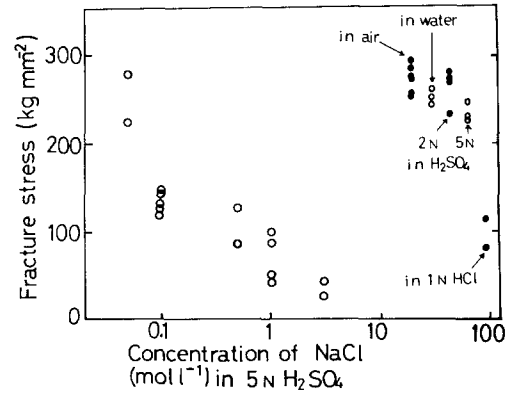

Figure 31 Variation of fracture stress of Fe–7Cr–20Ni–14P–6C alloy as a function of NaCl concentration in 5 N H_2SO_4 at the corrosion potential and at a strain-rate of 5.6×10^{-6} sec^{-1} [34].

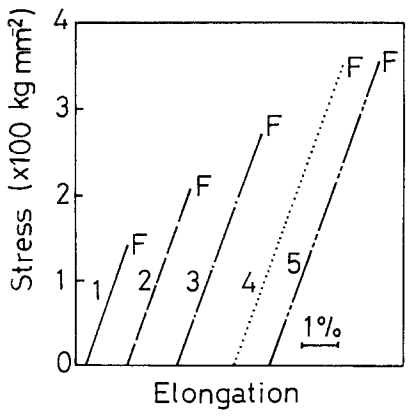

Figure 33 Tensile stress–elongation curves measured in air of amorphous Fe–7Cr–20Ni–14P–6C alloy treated differently after cathodic polarization for 1 h at 12 mA cm^{-2} in 2 N H_2SO_4. Strain-rate = 5.6×10^{-6} sec^{-1}. Symbol F denotes fracture of specimen [34]. Tensile measurements taken (1) after 5 min at room temperature, (2) after 1 h at room temperature, (3) after heating at 100° C for 40 h or for 2 h in vacuum (10^{-6} torr), (4) in liquid N_2 for a hydrogen-free specimen and (5) in liquid N_2 for a hydrogenized specimen.

may be attributed to hydrogen embrittlement resulting from diffusion of absorbed hydrogen. A similar conclusion has also been reported with respect to the embrittlement behaviour of metallic glasses in the passive region during tests under various conditions, for sample in the work of Pampillo [34] regarding the Ni–$Fe_{29}P_{14}B_6Al_2$ glass.

Metallic glasses containing a certain concentration of Cr and P have been made which show extremely high corrosion resistance both under static and dynamic conditions, when compared with presently available crystalline stainless steel [36]. For these glasses, tensile specimens exposed to corrosion-active liquids such as sea-water do not show evidence of stress corrosion cracking. However, metallic glasses clearly show the susceptibility to hydrogen embrittlement as noted in this section. For this reason, hydrogen embrittlement, occurring either in the presence of Cl^- ions in solution of due to hydrogen, is one of the important research subjects in the study of the corrosion of metallic glasses.

8. Concluding remarks

Some metallic glasses possess superior corrosion-resistance properties to those of crystalline stainless steels. In particular, the immunity to pitting corrosion in HCl solution is one of the most interesting characteristics of metallic glasses. The addition of Cr and P to iron-base glasses is especially effective; this is attributed to the rapid formation of a uniform, stable, passive film with a high protective quality.

The high reactivity of metallic glasses rapidly accumulates beneficial elements in the surface film and hence leads to the *rapid* formation of passive film as well as to the strong tendency for spontaneous passivation even in aggressive hydrochloric acid solutions. Large amounts of P in metallic glasses accelerate the active dissolution prior to the passive film formation. This results both in the rapid enrichment of passivating species such as chromic ions in the bulk material–solution interface and in the rapid formation of a passive film. Thus, hydrated chromium oxyhydroxide is obtained in metallic glasses containing P and Cr as constituents.

The formation of a *uniform* passive film is associated with the low density of active surface sites due to the chemically homogeneous single-phase nature of metallic glasses and due to the absence of crystalline defects such as grain boundaries. However, elemental composition is a critical factor in determining their corrosion behaviour since several metallic glasses exhibit poor corrosion-resistance properties. In addition, metallic glasses have been shown to be susceptible to hydrogen embrittlement.

TABLE V Amount of hydrogen absorbed (ppm) [35]

Environment	Hydrogen absorbed (ppm)				
	Unstressed*			Stressed†	
	$E = 0$	$E = E_{corr}$	$E = -500$ mV	$E = E_{corr}$	$E = +500$ mV
Air	18.0				
5 N H_2SO_4				37.2	37.8
5 N H_2SO_4 + 0.5 N NaCl		25.4	138.3	43.3	52.4
5 N H_2SO_4 + 3 N NaCl		28.4			

*Unstressed specimens were exposed for 2 h at corrosion potential and for 1 h at −500 mV.
†Traction of specimens was performed up to a stress of about 110 kg mm^{-2} for about 1.5 h in solutions.

An extremely high corrosion resistance observed for the metal–metalloid-type glasses is not seen for alloy glasses of the metal–metal-type containing no metalloid elements. However, the addition of a small amount of a metalloid such as P to metal–metal-type glasses remarkably improves their corrosion resistance. Studies on the corrosion behaviour of metallic glasses also give valuable information which can be applicable to the improvement of the crystalline corrosion-resistant alloys. Such applicability has been demonstrated by the rapid-quenched crystalline Ti–Ni alloy having a single-phase solid solution.

Acknowledgements

The authors wish to acknowledge the valuable suggestions and encouragement of Professor T. Masumoto, who also provided his interesting results including those prior to publication. His pioneer studies on the corrosion behaviour of metallic glasses also gave the incentive for writing the present article. The financial support from the Natural Science and Engineering Council of Canada is gratefully acknowledged. One of the authors (YW) also expresses thanks to the Ito Science Foundation and the RCA Research Laboratories (Japan) for the provision of grants in 1979–80.

References

1. W. KLEMENT, R. H. WILLENS and P. DUWEZ, *Nature* **187** (1980) 869.
2. H. J. LEAMY and J. J. GILMAN, (Eds.) "Metallic Glasses", (American Society for Metals, Metals Park, Ohio, 1978).
3. M. NAKA, K. HASHIMOTO and T. MASUMOTO, *J. Japan Inst. Met.* **38** (1974) 835.
4. Y. WASEDA and K. T. AUST, unpublished work 1980.
5. K. HASHIMOTO, M. KASAYA, K. ASAMI and T. MASUMOTO, *Corros. Eng. (Boshoku Gijutsu)* **26** (1977) 445, in Japanese.
6. M. NAKA, K. HASHIMOTO, K. ASAMI and T. MASUMOTO, in Proceedings of the 3rd International Conference on Rapidly Quenched Metals, Brighton, July, 1978, edited by B. Cantor (The Metals Society, London, 1978) p. 449.
7. C. M. HANHAM, Y. WASEDA and K. T. AUST, *Mater. Sci. Eng.* **45** (1980) 71.
8. B. CANTOR (Ed.), Proceedings of the 3rd International Congress on Rapidly Quenched Metals, Brighton, July, 1978 (The Metals Society, London, 1978).
9. K. ASAMI, K. HASHIMOTO, T. MASUMOTO and S. SHIMODAIRA, *Corros. Sci.* **16** (1976) 909.
10. M. NAKA, K. HASHIMOTO and T. MASUMOTO, *Sci. Rep. Inst. Tohuku Univ.* **A26** (1977) 283.
11. K. HASHIMOTO, K. OSADA, T. MASUMOTO and S. SHIMODAIRA, *Corros. Sci.* **16** (1976) 71.
12. R. B. DIEGLE, *Corrosion NACE* **35** (1979) 250.
13. G. RIFE, P. C. C. CHAN, Y. WASEDA and K. T. AUST, *Mater. Sci. Eng.* **48** (1981) 73.
14. K. HASHIMOTO, M. NAKA, J. NOGUCHI, K. ASAMI and T. MASUMOTO, in Proceedings of the 4th International Symposium on the Passivity of Metals, Airlie, Virginia, October, 1977, edited by R. P. Frankenthal and J. Kruger (Electrochemical Society, Princeton, New Jersey, 1978) p. 156.
15. K. HASHIMOTO, *Corros. Eng. (Boshoku Gijutsu)* **28** (1979) 351, in Japanese.
16. M. NAKA, K. HASHIMOTO and T. MASUMOTO, *J. Non-cryst. Sol.* **31** (1979) 355.
17. K. HASHIMOTO, *Bull. J. Japan Inst. Met.* **18** (1979) 362.
18. K. SUGIMOTO and Y. SAWADA, *Corros. Sci.* **17** (1977) 425.
19. K. HASHIMOTO, M. NAKA and T. MASUMOTO, *Sci. Rep. Res. Inst. Tohoku Univ.* **A26** (1976) 48.
20. M. NAKA, K. HASHIMOTO and T. MASUMOTO, *J. Non-cryst. Sol.* **28** (1978) 403.
21. K. HASHIMOTO, M. NAKA, K. ASAMI and T. MASUMOTO, *Corros. Eng. (Boshoku Gijutsu)* **27** (1978) 279, in Japanese.
22. *Idem, ibid.* **30** (1978) 29.
23. K. ASAMI, K. HASHIMOTO and S. SHIMODAIRA, *Corros. Sci.* **18** (1978) 151.
24. K. TERAMOTO, K. ASAMI and K. HASHIMOTO, *Corros. Eng. (Boshoku Gijutsu)* **27** (1978) 57, in Japanese.
25. G. OKAMOTO, *Corros. Sci.* **13** (1973) 471.
26. K. HASHIMOTO, M. NAKA, K. ASAMI and T. MASUMOTO, *Corros. Sci.* **19** (1979) 165.
27. V. BRUSIC, R. D. MacINNES and J. ABOAF, in Proceedings of the 4th International Symposium on the Passivity of Metals, Airlie, Virginia, October, 1977, edited by R. P. Frankenthal and J. Kruger (Electrochemical Society, Princeton, New Jersey, 1978) p. 170.
28. L. LEY and J. P. RILEY, in Proceedings of the 7th International Vacuum Congress and the 3rd International Conference on Solid Surfaces, Vienna, September, 1977, Vol. III, edited by R. F. Rudenauer, F. P. Viehbock and A. Breth, p. 2031; Metals Abstracts, September, 1978, p. 1616.
29. M. NAKA, K. ASAMI, K. HASHIMOTO and T. MASUMOTO, Proceedings of the 4th International Conference on Titanium, Kyoto, 1980.
30. M. NAKA, K. HASHIMOTO and T. MASUMOTO, *Sci. Rep. Res. Inst. Tohoku Univ.* **A28** (1980) 156.
31. T. M. DAVINE, *J. Electrochem. Soc.* **124** (1977) 38.
32. H. S. CHEN, *Rep. Prog. Phys.* **43** (1980) 353.
33. A. KAWASHIMA, H. HASHIMOTO and T. MASUMOTO, in Proceedings of the 2nd International Conference on Rapidly Quenched Metals, Boston, Mass., November, 1975, edited by N. J. Grant and B. C. Giessen (MIT Press, Cambridge, Mass., 1976) p. 475.
34. C. A. PAMPILLO, *J. Mater. Sci.* **10** (1975) 1194.
35. A. KAWASHIMA, K. HASHIMOTO and T.

MASUMOTO, *Corros. Sci.* **16** (1976) 935.
36. D. E. POLK, B. C. GEISSEN and F. S. GARDNER, *Mater. Sci. Eng.* **23** (1976) 309.
37. K. HASHIMOTO, K. ASAMI and K. TERAMOTO, *Corros. Sci.* 19 (1979) 3.
38. K. HASHIMOTO and K. ASAMI, *ibid.* **19** (1979) 251.

Received 9 January and accepted 5 February 1981.